ARTICLE

OBC
www.rsc.org/obc

Translational isomerism and dynamics in multi-hydroquinone derived porphyrin [2]- and [3]-catenanes

Maxwell J. Gunter,* Sandra M. Farquhar and Tyrone P. Jeynes
Chemistry, School of Biological, Biomedical and Molecular Sciences, University of New England, Armidale, NSW 2351, Australia.
E-mail: mgunter@pobox.une.edu.au; Fax: 612 6773 3268; Tel: 612 6773 2767

Received 21st July 2003, Accepted 12th September 2003
First published as an Advance Article on the web 7th October 2003

A series of porphyrins strapped with polyether chains containing two or three 1,4-dioxybenzene units has been synthesised with a view to the production of porphyrin-containing [2] and [3]catenanes, where the porphyrin is strapped between *ortho*-positions of 5,15-(*meso*)-diaryl groups, and is interlinked with the bipyridinium macrocycle cyclo*bis*(paraquat-4,4′-biphenylene). The porphyrins were isolated as mixtures of atropisomers, where the linking strap spans across the face of the porphyrin (α,α-isomer), or 'twisted' around its side (α,β-isomer). Their structures were determined by detailed ^{1}H NMR spectroscopy. The *bis*-1,4-dioxybenzene-strapped derivatives were shown to undergo atropisomerisation on heating, to produce an equilibrium mixture. Catenation under high pressure conditions of the mixture, or of the individual isomers, produced only a single catenane, that of the α,α-isomer. Its structure was determined by mass spectral and dynamic NMR measurements. Rates were determined for: (i) translational motion or 'shuttling' between 1,4-dioxybenzenes; (ii) 'rotation' of the macrocycle around the 1,4-dioxybenzene axis; and (iii) 'rocking' of the 1,4-dioxybenzene within the macrocycle. The atropisomers of the strapped derivatives containing *three* 1,4-dioxybenzene units were also separated, and subjected to catenation. Both [2]- and [3]catenanes were isolated, and were shown to be stable to further atropisomerisation. Their solution structures were probed in detail by dynamic ^{1}H NMR measurements. The rates for shuttling and rotation were obtained in certain cases, although the complexity of the spectra of the [3]catenanes prevented a more detailed investigation.

Introduction

The concept of using a catenane as a molecular device,[1] or as a component of a molecular-scale machine[2–4] depends critically on the ability to exercise precise control over its dynamics, such as those involving translational motion. This can be achieved to some extent by design, relying on differential thermodynamic stability between isomers,[5–7] or by higher order catenanes where one component undergoes a degenerate translational between equivalent sites;[6,8,9] this is in essence the principle of molecular 'trains' or 'shuttles'. In a more sophisticated approach, translational isomerism can be deliberately controlled by external stimuli such as protonation, electrochemistry, or photochemistry, for example. In these cases, the catenane is required to have an in-built addressable component.[4,10,11] Porphyrins provide a particularly useful range of controlled functionality that can be accessed through chemical, electrochemical, or photochemical means, and there have been several examples where these are incorporated into catenated structures.[12–16]

We have previously reported a series of strapped-porphyrin [2]catenanes **1a** and have examined in some detail the effects on the dynamics, chemical and photophysical behaviour as both the chain length of the strap and the nature of the central π-donor unit (1,4-dioxybenzene or 1,5-dioxynaphthalene) were varied.[14–17] Indeed such variations proved to have a profound influence on the observed dynamic behaviour of the catenanes as evidenced by the wide range in the calculated thermodynamic parameters for the diethylene to tetraethylene series of strapped porphyrin catenanes.[13,18]

Although the [2]catenanes prepared thus far exhibit interesting dynamic properties, their movement is restricted to rotation of the tetracationic cyclophane around the 1,4-dioxybenzene or 1,5-dioxynaphthalene axis, sometimes accompanied by a stretching of the porphyrinic link of the catenane, as observed in protonation studies.[16] We now wished to extend the range of molecular dynamics that might be possible in these systems by introducing a further degree of freedom, *viz* translational motion[7,19] in the resultant porphyrin catenanes. To this end, the synthesis of strapped-porphyrins which contain two (2HQ) and three (3HQ) hydroquinone-derived π-donor units, capable of forming catenanes, was seen as a logical extension. It was envisioned that in subsequent protonation or photochemical studies in these catenanes that the tetracationic cyclophane could be driven between 1,4-dioxybenzene 'stations', effectively acting as a molecular 'shuttle', which has been well illustrated in the work of Stoddart[2,7,8,11,20] for simpler non-porphyrinic systems derived from the classic BPP34-C-10-[2]catenane system **1b**. In our systems however, the porphyrin subunit provides an ideal trigger for control of the dynamics, as it can be addressed by chemical, photochemical, or electrochemical stimuli.

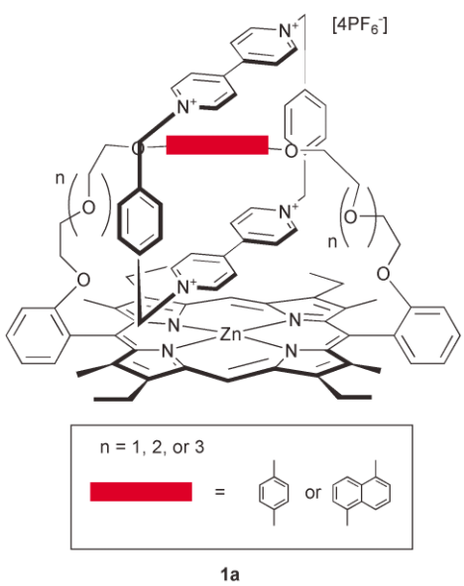

1a

DOI: 10.1039/b308157e

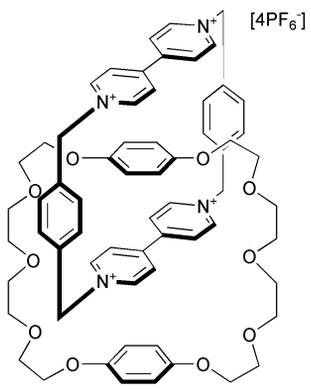

1b

In these strapped-porphyrins (Scheme 1), the polyether strap that we have chosen incorporates two and four ethyleneoxy units in symmetrical combinations (*ie*, 2,4,2 in the case of **7** and 2,4,4,2 in the case of **12**) between the porphyrin and the 1,4-dioxybenzene units. While this introduces a degree of asymmetry in the 1,4-dioxybenzene ring protons closest to the porphyrin, it still allows for some interaction between the porphyrin and the tetracationic macrocycle as we have found in previous studies.[15]

Furthermore, strapped porphyrins containing two or three hydroquinone-derived units have the potential to undergo self-assembly of higher order porphyrin [3]catenanes using Stoddart's templating methodology.[19,21]

Results and discussion

(a) Strapped-porphyrins containing two (2HQ) and three (3HQ) hydroquinone-derived rings

Synthesis. The synthesis of the polyether strapped-porphyrins **7** and **10** containing two and three 1,4-dioxybenzene rings (2HQ and 3HQ) is outlined in Scheme 1 and follows a similar methodology to that employed for the synthesis of previously reported [15,22,23] strapped-porphyrins. The dialdehydes **4** and **10** were produced from the corresponding 1,4-dioxybenzene polyethers [7] as indicated in Scheme 1. The dialdehyde derivatives were then condensed with dipyrrylmethane **5** by trichloroacetic acid catalysis using a modification of Maruyama's procedure,[24] (with the addition of Cs_2CO_3 [25] as template in the case of the longer dialdehyde **10**), followed by oxidation of the porphyrinogen with *o*-chloranil to give the desired porphyrin products. As we have previously observed for longer 1,4-dioxybenzene- and 1,5-dioxynaphthalene-containing tetraethylene strapped-porphyrins,[23] and others for related long-strapped porphyrin derivatives,[26] the synthesis resulted in a mixture in each case of both 'twisted' strapped or α,β-isomers and the atropisomeric 'over-the-face' α,α-isomers; in these cases the α,α-**7a** and its α,β-isomer **6a** in 7% and 15% yields, respectively, and for the longer 3HQ analogue, the α,α-isomeric porphyrin **12a** in 4% yield and its statistically more favoured α,β-isomer **11a** in 14%.

The two atropisomers in each case could be separated chromatographically, but each of the individual isomers interconverted in refluxing acetonitrile solution by rotation of the *meso*-phenyl ring about the C(9)–(10) axis (see Scheme 1 for the simplified numbering system), to form a 1:5 equilibrium mixture of **6a** and **7a**, or a 3:2 mixture of **11a** and **12a**. Confirmation that these two sets of porphyrins are isomeric was also provided by electrospray mass spectrometry (ESMS) where both free base isomers **6a** and **7a** showed peaks at *m*/*z* 1182.1 (calcd 1181.6) $[M]^+$, and at 591.6 (calcd 591.3) $[M]^{2+}$. Similar results confirmed the isomeric relationship of the porphyrins containing the three hydroquinone-derived rings **11a** and **12a** (peaks at 1450.4 (calcd 1449.7) $[M]^+$, and 725.7 (calcd 725.4) $[M]^{2+}$. In addition, each pair of isomers have virtually identical UV-vis spectra for both free base and zinc derivatives.

Table 1 ^{1}H NMR resonance assignments for the free base porphyrin isomers containing 2HQ (**6a** and **7a**) or 3HQ rings (**11a** and **12a**) recorded at 300 MHz in $CDCl_3$ at 298 K

Position	6a	7a	11a	12a
1	10.14	10.17	10.20	10.21
4	3.92	3.98	4.00	4.01
5	1.70	1.75	1.77	1.79
7	2.54	2.56	2.59	2.60
pyrrole NH	−2.36	−2.34	−2.27	−2.25
11	7.77	7.75	7.79	7.79
12	7.36	7.35	7.40	7.39
13	7.74	7.77	7.82	7.80
14	7.29	7.30	7.34	7.34
16	4.15	4.16	4.17	4.18
17	3.20	3.12	3.20	3.10
18	2.19	2.23	2.06	2.07
19	2.19	2.32	1.63	1.72
HQ-21	5.94	5.94	5.20	5.24
HQ-22	6.44	6.37	5.86	5.84
24	4.00	3.82	3.70	3.62
25	3.85	3.70	3.70	3.70
26	3.80	3.61	3.70	3.62
27	3.80	3.61	3.70	3.62
28	—	—	3.70	3.62
29	—	—	3.70	3.62
30	—	—	3.87	3.70
31	–	—	4.10	3.80
HQ-33	—	—	6.89	6.54

However, the ^{1}H NMR spectra of each isomer are distinctive. The spectra of the free base porphyrin isomers **6a** and **7a**, as well as **11a** and **12a**, were assigned by a combination of gradient COSY and NOESY two dimensional NMR experiments; the data are collected in Table 1, and the non-systematic numbering systems employed for the assignments of the ^{1}H NMR spectra are shown in Scheme 1.

Comparison of the ^{1}H NMR resonances of the open chain bis-hydroxy crown ethers **2** or **8** from which the free base porphyrin **7a** or **12a** are formed shows that the methylene protons of the polyether chain, and the 1,4-dioxybenzene ring protons (shielded $\Delta\delta$ −0.88 and −0.45 for **7a**, and $\Delta\delta$ −1.59, −1.29, and −0.26 for **12a**), undergo significant upfield shifts on porphyrin formation (Table 1), indicative of the ether chain strapping the porphyrin ring. Presumably, the extra shielding observed in **12a** over that for **7a** reflects the increased flexibility provided by the third 1,4-dioxybenzene ring and longer polyether strap, resulting in HQ-21 and HQ-22 being more centrally located over the porphyrin macrocycle.

Also of interest are the chemical shift changes of the polyether chain and 1,4-dioxybenzene ring protons for the α,β-isomers **6a** and **11a** compared to their α,α-isomers **7a** and **12a**. However, as expected the differences in resonances between isomers is not as pronounced in the more flexible longer strapped molecules in comparison to their shorter strapped analogues.

Significant differences in ^{1}H NMR chemical shifts between the two atropisomers which support the structures shown are as follows:

(i) 2HQ porphyrins **6** and **7**

• the hydroquinone-derived (HQ-22) ring proton of **6a** at 6.44 ppm is deshielded by +0.07 ppm compared to that in **7a**;

• the methylene protons of the polyether strap are shifted downfield in the α,β-isomer **6a** ($\Delta\delta$ +0.18, +0.15, +0.19, +0.19 ppm for H-24, -25, -26 and -27, respectively) compared to the α,α-isomer **7a**, as a result of being deshielded on twisting around the side of the porphyrin;

• the H-18 and H-19 protons are shifted upfield in **6a** compared to **7a** ($\Delta\delta$ −0.04 and −0.13 ppm, respectively), indicating shielding by the porphyrin as a result of being held closer to the

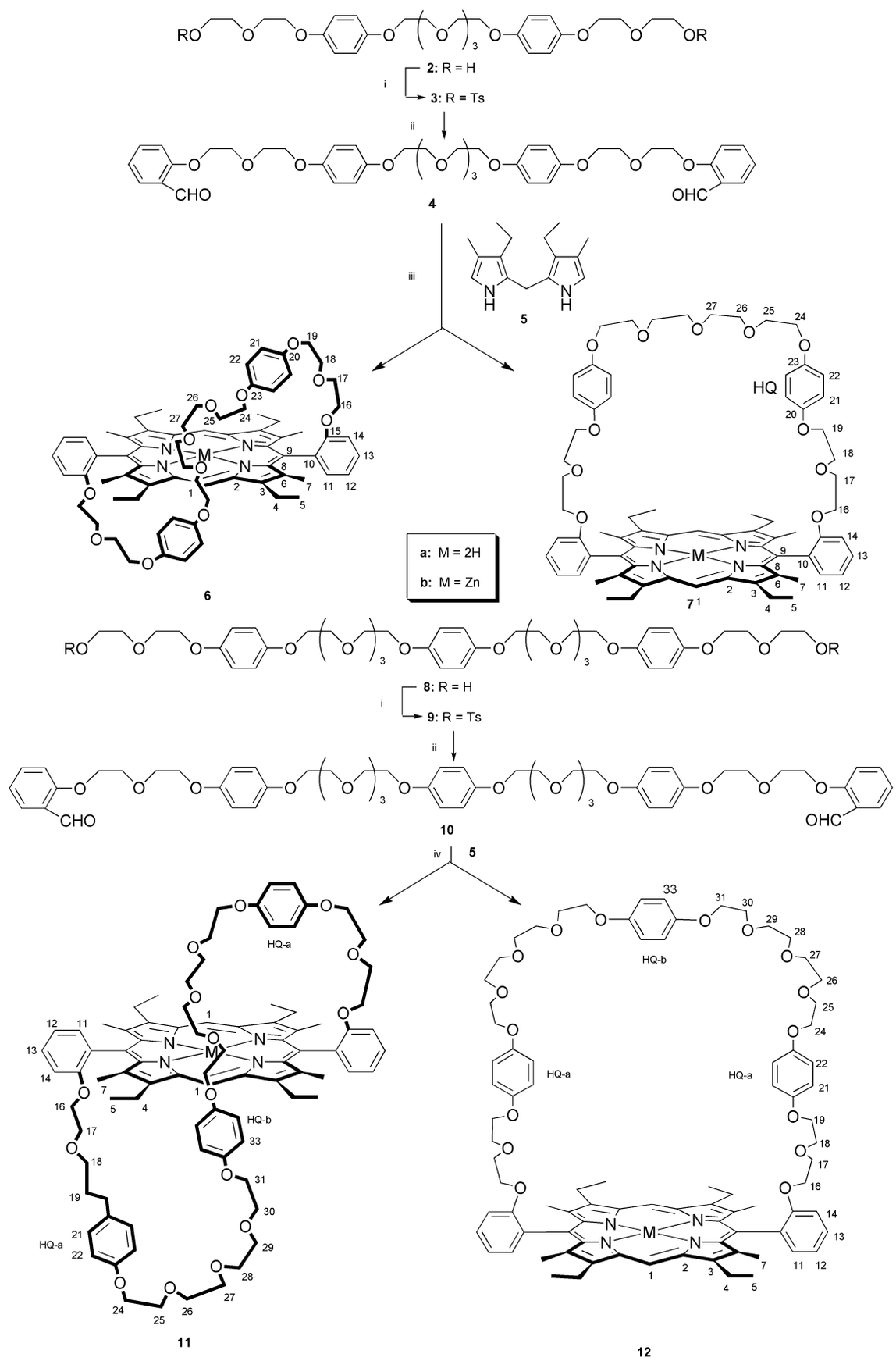

Scheme 1 *Reagents and conditions*: (i) *p*-toluenesulfonyl chloride, Et_3N, CH_2Cl_2; (ii) salicylaldehyde, K_2CO_3, MeCN; (iii) CCl_3CO_2H, MeCN–THF, then *o*-chloranil, then ZnOAc/MeOH/CH_2Cl_2 for **1b** (iv) CCl_3CO_2H, Cs_2CO_3, MeCN–THF, then *o*-chloranil, then ZnOAc/MeOH/CH_2Cl_2 for **1b**.

porphyrin nucleus as the strap is twisted around from one face to the other.

(ii) 3HQ porphyrins **11** and **12**

• the HQ-21 and HQ-22 protons are only slightly shifted from one isomer to the other, ($\Delta\delta$ −0.04 and +0.02 ppm, respectively) as expected, whereas the HQ-33 proton is significantly deshielded by +0.35 ppm in **11a**, indicating that the HQ-33 ring is held at the *side* of the porphyrin;

• the methylene protons in **11a** are shifted only slightly downfield ($\Delta\delta$ +0.08, 0.00, +0.08, +0.08 ppm for H-24 to H-27, respectively) upon twisting, reflecting the reduced influence of the porphyrin in the longer strapped analogues compared to the shorter strapped **6a**;

• the H-18 and H-19 protons in **11a** are shielded ($\Delta\delta$ −0.01 and −0.09 ppm, respectively), but as expected not to the same extent as for the tighter strapped **6a**. On the other hand, the methylene protons of the strap adjacent to the central HQ-33 ring (H-30 and H-31) are most affected by atropisomerisation ($\Delta\delta$ +0.17 and +0.30 ppm, respectively, from **12a** to **11a**), indicating that these protons are held closest to the side of the porphyrin ring and hence deshielded.

Interesting comparisons can also be made between the porphyrin isomers containing 2HQ and 3HQ rings (Fig. 1 and Table 1). Generally speaking, the methylene strap and HQ ring protons in the longer strapped derivatives (3HQ) resonate further upfield in the ^{1}H NMR, especially for the HQ-21 and HQ-22 protons and their adjacent methylene strap protons either side of the HQ-21,22 ring. For example, a comparison of the chemical shifts of the 'twisted' isomers **11a** and **6a** (Table 1 and Fig. 1), shows that the methylene strap protons, H-18, -19, -24 and -25 ($\Delta\delta$ −0.13, −0.56, −0.30, −0.15 ppm), as well as the HQ-21 and HQ-22 ring protons ($\Delta\delta$ −0.74, −0.58 ppm) resonate significantly further upfield in **11a**. Similar trends are also observed for the α,α-isomers **12a** and **7a**, with the equivalent methylene strap protons ($\Delta\delta$ −0.16, −0.60, −0.20, 0.00 ppm) and HQ ring protons ($\Delta\delta$ −0.70, −0.53 ppm) resonating further upfield in the longer strapped **12a** analogue. However, in contrast to the above observations, inspection of Table 1 reveals that the peripheral methyl and ethyl substituents of the porphyrin, as well as the *meso*-phenyl ring protons are all shifted further downfield in the 3HQ porphyrin series in comparison to the 2HQ porphyrin isomers. These two opposing trends indicate that the HQ-21 and HQ-22 rings are held closer to the peripheral groups in the tighter strapped 2HQ isomers, whereas in the 3HQ porphyrins the inherent flexibility provided by the third HQ ring and additional polyether chain allows the HQ-21 and HQ-22 protons to be more centrally located over the porphyrin face.

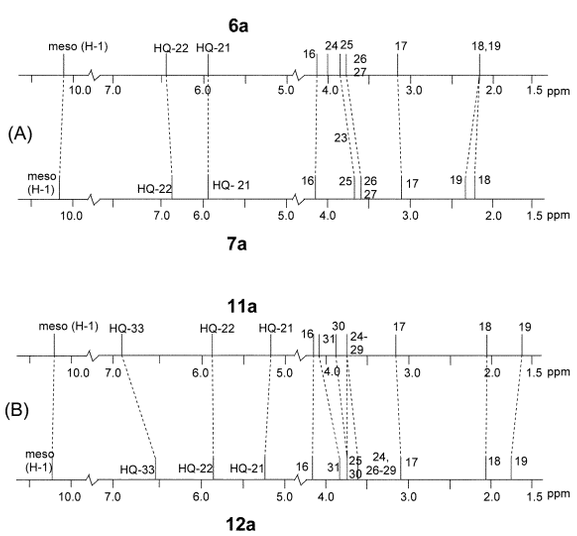

Fig. 1 Schematic representation of the differences in the chemical shifts of the "twisted" α,β-strapped porphyrins compared to the α,α-porphyrins: (A) **6a** compared to its α,α-strapped atropisomer **7a**; (B) **11a** compared to its α,α-strapped atropisomer **12a**.

(b) [*n*]Catenane self-assembly

(i) [2]catenanes from 2HQ porphyrins 6 and 7. *Synthesis.* The synthesis of the porphyrin catenanes is shown in Scheme 2 and employs a similar methodology and workup procedure to that used previously for the porphyrin [2]catenanes containing

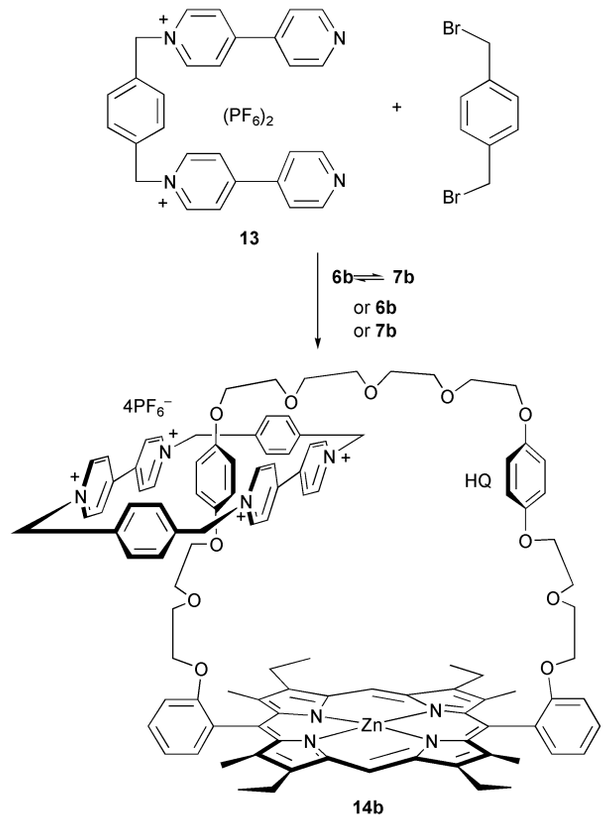

Solvent	Pressure	Days	Molar Equiv. 13	Molar Equiv. di-Br xylene	Yield
DMF	Ambient	17	1.2	1.5	1%
DMF	12 kbar	3	1.2	1.5	20%
DMF	12 kbar	3	3	3.75	40%

Scheme 2 Self-assembly of a strapped-porphyrin [2]catenane **14b** containing two hydroquinone-derived rings (2HQ) in DMF under various reaction conditions. Yields improved substantially under high pressure conditions (12 kbar), and with excess reagents.

one 1,4-dioxybenzene or 1,5-dioxynaphthalene unit.[13,15,23] Very low yields of catenated products were obtained at ambient temperature and pressure, but by use of high pressures[27] and using excess reagents, the yields were increased markedly (Scheme 2).

The 2HQ porphyrin [2]catenane **14b** was the only catenated product identified and isolated when either of the individual isomeric porphyrins **6b** or **7b**, or an equilibrated mixture of the two, was used. From examination of models, it is apparent that catenation of the 'twisted' isomer **6b** would be unlikely because of steric constraints. It is also significant however, that there was no evidence for a [3]catenane from this reaction, although molecular modelling suggests that it is sterically feasible, although unlikely if there were to be π–π interactions involving the porphyrin and the bipyridinium macrocycle (see below).

Electrospray mass spectrometry (ESMS) for the 2HQ [2]catenane **14b** showed a pattern which has come to be considered indicative of catenated structures,[19] where peaks were observed for the successive loss of one, two, three and four PF_6^- counterions, as well as peaks corresponding to the singly and doubly charged parent porphyrin ions, as a result of the breaking of the tetracationic macrocycle.

The assignment of the ^{1}H NMR resonances of the 2HQ strapped-porphyrin [2]catenane **14b** under conditions of fast or slow exchange was undertaken by a combination of gradient

COSY, gradient NOESY, selective gradient NOE and saturation transfer experiments. However, unlike previous porphyrin [2]catenanes,[15] no NOE interactions were observed between the protons of the bound 1,4-dioxybenzene and tetracation components. This may possibly be due to the extra exchange process available in **14b**, *viz* 'shuttling' or translational motion of the tetracation between 1,4-dioxybenzene units, in addition to the 'rocking' and rotation of the tetracation, exchange processes also observed in the single hydroquinone-derived catenanes. Nevertheless, the usual NOE interactions that we have observed between the protons of the tetracation cyclophane components in previous porphyrin [2]catenanes were evident here in **14b** and allowed us to unambiguously assign these resonances.[14–17] Furthermore, saturation transfer experiments, together with gradient COSY and NOESY experiments were used to assign the 'inside' and 'outside' 1,4-dioxybenzene (HQ) environments (Table 2) in both $(CD_3)_2CO$ and CD_3CN solution at 30 °C. In addition, four separate signals corresponding to the protons H-16,16′ and H-17,17′ of the polyether chain were observed. This indicates that shuttling between the two possible 1,4-dioxybenzene units of this catenane is slow on the NMR time scale at this temperature, and confirms the structure as that of a [2]catenane **14b**.

Selected ^{1}H NMR resonances for **14b** recorded in $(CD_3)_2CO$ or CD_3CN solution at 30 °C are shown in Table 2. For comparison, ^{1}H NMR chemical shifts for the tetraethylene strapped 1,4-dioxybenzene porphyrin [2]catenane (**1a**:n = 3), as well as ^{1}H NMR data for the BPP34C10-[2]catenane[27] **1b** are included in Table 2. Like the previously reported porphyrin [2]catenanes,[15] the resonances of tetracation cyclophane components in **14b** have an increased chemical shift difference in comparison to **1b**, due to the influence of the large magnetic anisotropy of the porphyrin macrocycle. Furthermore, as observed for previous[15] porphyrin [2]catenanes the ^{1}H NMR resonance shifts for **14b** support a structure in which the bipyridinium moiety, bound 1,4-dioxybenzene and porphyrin subunits are held co-parallel (Fig. 2). For example, both the β- and α-bipyridinium protons in $(CD_3)_2CO$ solution for **14b** ($\Delta\delta$ −1.85 and −1.09 ppm, respectively) are more affected by catenane formation then either the $^+NCH_2$ or phenylene (–C_6H_4–) protons ($\Delta\delta$ −0.84 and −0.70 ppm, respectively); similar trends are also observed in CD_3CN solution at 30 °C (Table 2). As before, this implies that both the β- and α-bipyridinium protons of the bipyridinium subunit are held closest to the porphyrin, and are therefore most affected by the porphyrin ring current. Also, the larger chemical shift difference experienced by the β-bipyridinium protons upon catenane formation reflects the more centralised position of these protons above the porphyrin.

Furthermore, the changes in chemical shift for the tetracation and 1,4-dioxybenzene units upon catenation are of a similar magnitude to that observed for (**1a**:n = 3) (Table 2), with the exception of the phenylene (–C_6H_4–) resonance, which is shifted further upfield in **14b** ($\Delta\delta$ −0.70 ppm) compared to (**1a**:n =3) ($\Delta\delta$ −0.33 ppm), and reflects the extra shielding influence of the second hydroquinone-derived (HQ) unit in **14b**. Also, the change in chemical shift for the HQ (H-21 and -22) ring protons in **14b** for the 'inside' or bound protons ($\Delta\delta$ −3.27 and −3.42 ppm, respectively) in $(CD_3)_2CO$ solution are of a similar magnitude to those in both (**1a**:n =3) ($\Delta\delta$ −3.12 ppm) and **1b** ($\Delta\delta$ −3.01 ppm), further supporting the catenated structure. The downfield shifts observed for 'outside' or unbound HQ-21 and HQ-22 ring protons on catenation ($\Delta\delta$ +0.58 and +0.29 ppm, respectively), as opposed to upfield shift in the 'outside' or 'alongside' HQ protons in **1b** ($\Delta\delta$ −0.55 ppm), imply that the second HQ unit undergoes a conformation induced change in which this ring is moved away from the effects of the porphyrin to allow π–π interactions to occur between the bipyridinium moiety, the first 1,4-dioxybenzene and the porphyrin subunits, as indicated in Fig. 2. The pattern of chemical shifts clearly does not support an alternative structure **14′** which would require close approach of the phenylene groups on the macrocycle to the porphyrin ring.

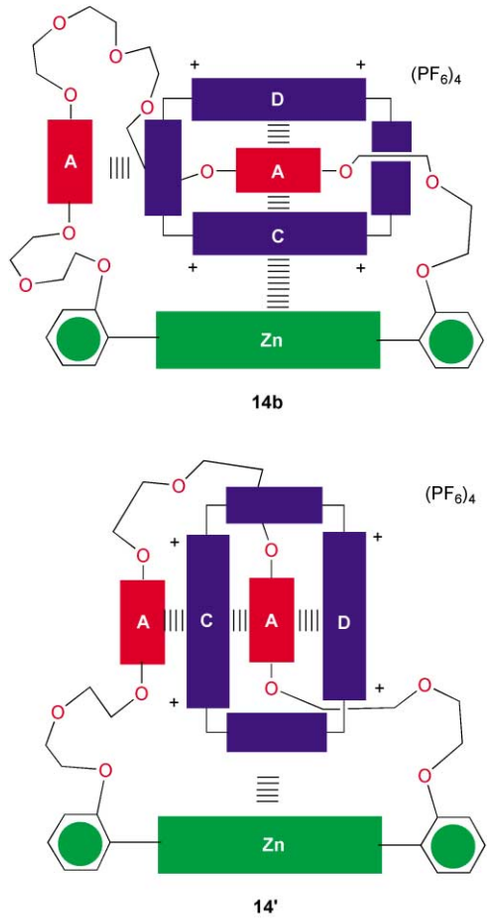

Fig. 2 Cartoons indicating the possible conformations of the catenane **14b**; conformation **14′** is not supported by NMR evidence (see text).

Dynamic ^{1}H NMR. Several different exchange processes were identified for **14b** in solution over a wide temperature range, and selected ^{1}H NMR chemical shifts under conditions of both fast and slow exchange are collected in Table 3. The data were evaluated using the coalescence method[28] to determine the kinetic and thermodynamic parameters (Table 4).

Further evidence for slow translational isomerism at 30 °C in either CD_3CN or $(CD_3)_2CO$ solution for the 2HQ porphyrin [2]catenane **14b** (besides the distinct 'inside' and 'outside' HQ resonances) were signals corresponding to the H-16,16′ protons of the polyether strap, two singlets for the methyl groups of the porphyrin periphery (H-7), and two doublets corresponding to the diastereotopic $^+NCH_2$ protons of the tetracationic macrocycle.

On raising the temperature in CD_3CN solution all these resonances began to broaden and at 70 °C the HQ resonance had disappeared; no peaks corresponding to the fast exchange limit were observed for the HQ ring protons. Nevertheless, by monitoring the coalescence of the porphyrin peripheral methyl (H-7) and H-16,16′ and $^+NCH_2$ resonances, the translational motion of the tetracation was found (Table 4) to have $k_c = 23\ s^{-1}$ at T_c of 50 °C in CD_3CN ($\Delta\nu$ 10.4 Hz) with a $\Delta G^{\ddagger}_c$ of 70.7 kJ mol^{-1}, which converts to around 1.3 times per second at 25 °C. Hence the rate of translational motion between HQ 'stations' in this catenane is slow, and is about two orders of magnitude slower than that found by Stoddart[8,27] for the BPP34C10-[2]-catenane **1b** of *ca.* 120 s^{-1} at ambient temperature ($\Delta G^{\ddagger}_c$ 65.3 kJ mol^{-1}), and reflects both the increased activation barrier for translational motion imposed by the presence of the porphyrin and the statistical difference arising from restriction to a back-and-forth mode in these catenanes *vs.* full-circle possibilities in

Table 2 Selected ^{1}H NMR resonances (δ ppm) and chemical shift differences ($\Delta\delta$ ppm) for the 2HQ porphyrin [2]catenane **14b**, isomeric 3HQ α,β-**16b** and α,α-**15b** [2]catenanes, and isomeric 3HQ α,β-**18b** and α,α-**17b** [3]catenanes

	α	β	$-C_6H_4-$	$^+NCH_2$	outside HQ-21	outside HQ-22	inside HQ-21	inside HQ-22	HQ-33
Macrocyclic tetracation[a]	9.38	8.58	7.76	6.15					
Macrocyclic tetracation[b]	8.85	7.66	7.79	5.67					
1b (BPP34C10 [2]catenane)[a]	9.28	8.18	8.04	6.01		6.22	3.76		
($\Delta\delta$)[c]	(−0.10)	(−0.40)	(+0.28)	(−0.14)		(−0.55)	(−3.01)		
1:n = 3[d]	8.28	6.66	7.43	5.29			3.00		
($\Delta\delta$)[c]	(−1.10)	(−1.92)	(−0.33)	(−0.86)			(−3.12)		
7b[e]					5.98	6.44			
14b[f]	8.29	6.73	7.06	5.31	6.56	6.73	2.71[i]	3.02[i]	
($\Delta\delta$)[c]	(−1.09)	(−1.85)	(−0.70)	(−0.84)	(+0.58)	(+0.29)	(−3.27)	(−3.42)	
14b[g]	7.71	5.99	7.10	5.03/4.77	6.68	6.91	2.36	2.69	
($\Delta\delta$)[c]	(−1.14)	(−1.67)	(−0.69)	(−0.64/–0.90)	(+0.70)	(+0.47)	(−3.62)	(−3.75)	
11b[e]					5.34	6.06			6.88
16b[h]	8.19	6.44	7.56	5.36	6.22	6.22	3.44[j]	3.58[j]	6.32[k]/5.83[k]
($\Delta\delta$)[c]	(−1.19)	(−2.14)	(−0.20)	(−0.79)	(+0.78)	(+0.16)	(−1.90)	(−2.48)	(−0.56)/(−1.05)
12b[e]					5.48	6.06			6.60
15b[f]	8.12	6.08	7.32	5.36	6.85	7.05	2.58[i]	2.68[i]	6.94[k]
($\Delta\delta$)[c]	(−1.26)	(−2.50)	(−0.44)	(−0.79)	(+1.37)	(+0.99)	(−2.90)	(−3.38)	(+0.34)
18b[h]	8.70	7.24	7.64	5.49					—
($\Delta\delta$)[c]	(−0.68)	(−1.34)	(−0.02)	(−0.66)			—	—	—
17b[h]	8.63	7.17	7.61	5.49			—	—	—
($\Delta\delta$)[c]	(−0.75)	(−1.41)	(−0.05)	(−0.66)			—	—	—

[a] Macrocyclic tetracation is cyclo*bis*(paraquat-4,4′-biphenylene); data is from Stoddart *et al*.[19] and was recorded in $(CD_3)_2CO$. [b] Data is from Stoddart *et al*.[27] and was recorded in CD_3CN. [c] ($\Delta\delta$) represents the change in chemical shift on formation of the [2]catenane from its component parts, *viz*. macrocyclic tetracation and the corresponding crown ether, **1b** (BPP34C10), or strapped porphyrin containing 1HQ (**1**: n = 3), 2HQ **7b**, or 3HQ (α,β-**11b** and α,α-**12b**) units. [d] Spectrum recorded in $(CD_3)_2CO$ at 25 °C. [e] Recorded in $CDCl_3$ at 30 °C. [f] Recorded in $(CD_3)_2CO$ at 30 °C. [g] Recorded in CD_3CN at 30 °C. [h] Recorded in $(CD_3)_2SO$ at 60 °C; 'inside and 'outside' HQ resonances not assigned under slow exchange conditions, but identified at 90 °C under fast exchange, see text. [i] Identified by a saturation transfer experiment performed at 30 °C in $(CD_3)_2CO$. [j] Identified by gradient NOESY and COSY experiments performed at 30 °C in $(CD_3)_2CO$. [k] Refers to the 'outside' HQ-33 protons – the 'inside' HQ-33 protons hidden at 30 °C; 'inside' HQ-33 protons observed at δ 4.11 and 4.34 ppm at 70 °C in CD_3CN.

Table 3 Selected proton chemical shift values (δ ppm) for the 2HQ porphyrin [2]catenane **14b** under conditions of both fast and slow exchange[a]

^{1}H	Fast rotation, CD_3CN, 343 K	Slow rotation,[b] $(CD_3)_2CO$, 253 K	$\Delta\delta$[c]
α	7.75	'outside' 8.53 'inside' 8.07	0.46
β	6.17	'outside' 6.88 'inside' 6.19	0.69
$-C_6H_4-$	7.08	7.20	—
$^+NCH_2$	4.89	5.41 5.08	0.33
HQ-21	–[d]	'outside' 6.75 'inside' 2.87[e]	3.88
HQ-22	–[d]	'outside' 6.52 'inside' 2.64[e]	3.88
OCH_2 (H-16)	4.58	4.82 4.68	0.14
Me (H-7)	2.62	2.80 2.64	0.16

[a] Spectra were recorded at 300 MHz using the appropriate residual solvent as reference. [b] This is not the 'slowest' exchange limit, with a further splitting of the α resonances observed at temperatures below 208 K, which is attributed to the 'rocking' process observed in 1,4-dioxybenzene catenanes (see Table 4 and text) [c] Chemical shift differences ($\Delta\delta$ ppm) between protons in slow exchange environments. [d] Peaks disappeared at this temperature and were not identified. [e] Identified by saturation transfer techniques in $(CD_3)_2CO$ at 30 °C.

Table 4 Kinetic and thermodynamic parameters from the dynamic 1H NMR studies on the porphyrin [2]catenanes containing one (**1a**:n = 3), two (**14b**) and three (**16b** and **15b**) 1,4-dioxybenzene rings

Catenane	Probe protons	Solvent	$\Delta\nu$/Hz	T_c/°C	k_c/s^{-1}	Rotation rates at 25 °C/Hz	$\Delta G_c‡$/kJ mol^{-1}
1a:$n = 3$[b]	α-CH	$(CD_3)_2CO$	62	−80	138	3.4×10^5	39
14b[c]	$^+NCH_2$	CD_3CN	31	65	69	5.2×10^{-1}	71
14b[c]	OCH_2 (H-16)	CD_3CN	31.5	55	70	2.7	69
14b[c]	Me (H-7)	CD_3CN	10.4	50	23	1.3	71
14b[b]	α-CH	$(CD_3)_2CO$	108	3	241	7.0×10^2	55
14b[d]	α-CH	$(CD_3)_2CO$	38	−65	85	9.3×10^4	44
16b[c,e]	HQ-33[f]	CD_3CN	613	70	1926	3.5×10^1	63
15b[c,e]	HQ-33[f]	CD_3CN	828	70	2601	4.9×10^1	62

[a] Data obtained by the coalescence method[27] as previously reported.[15] [b] Refers to the spinning process of the tetracation around the 1,4-dioxybenzene unit and involves exchange of the bipyridinium units between 'inside' and outside' environments. [c] Refers to the 'threading' or translational motion of the tetracation between the 1,4-dioxybenzene units. [d] Refers to 'rocking' process of the 1,4-dioxybenzene unit between different orientations within the tetracation [e] Data obtained by the exchange method as described by Stoddart[27] [f] Assignment of the 'inside' and 'outside' environments by saturation transfer experiments was not unequivocal in **15b**, and not observed in **16b** (see text).

the non-porphyrinic analogues. Nevertheless, it indicates that translational motion in this catenane is either sterically restricted because of the short diethylene strap linking the porphyrin and the 2HQ rings, or may reflect a stronger π–π interaction between the tetracation, bound HQ ring, and porphyrin moieties, or a combination of both.

At lower temperatures in $(CD_3)_2CO$ solution two other dynamic processes were also observed. At temperatures below 30 °C in the ^{1}H NMR spectrum both the α- and β-bipyridinium resonances of the tetracation began to broaden, and then split into two equal intensity peaks at temperatures below *ca.* 0 °C. This is interpreted as an interchange of the bipyridyl rings (C and D in Fig. 2) between the 'inside' and 'outside' environments,[8,27] a process which can be considered as rotating of the tetracation about an axis created by the 1,4-dioxybenzene ring. This process was found (Table 4) to have $k_c = 241$ s^{-1} at T_c of 3 °C in $(CD_3)_2CO$ ($\Delta\nu$ 108 Hz) with a $\Delta G_c^‡$ of 55 kJ mol^{-1}, which equates to *ca.* 700 rotations per second at 25 °C. This value for the rotation of the tetracation is significantly smaller than that found for the tetraethylene strapped-porphyrin [2]catenane containing one HQ ring (**1a**: $n = 3$) (Table 4) (3.4×10^5 Hz), and the non-porphyrinic BPP34C10 [2]catenane[8,27] **1b** (2000 Hz), but is larger than the diethylene strapped-porphyrin [2]catenane containing one HQ ring (**1a**:$n = 1$) (50 Hz).[15] These trends indicate that the short diethylene straps linking the porphyrin and the 2HQ rings in **14b** cause a degree of steric restriction, despite the presence of the longer tetraethylene strap between the 2HQ rings.

Secondly, at temperatures below *ca.* −30 °C, the already split α- and β-bipyridinium resonances begin to broaden further still and disappear from the ^{1}H NMR spectrum at *ca.* −50 °C, as do the 'inside' HQ resonances. At temperatures below −60 °C the broadened α-bipyridinium resonances begin to reappear and split into two equal intensity 'outside' peaks (the two 'inside' α-bipyridinium resonances were hidden under several Ar–H protons at −85 °C at *ca.* 7.8 ppm) at temperatures below −65 °C before starting to sharpen again. These results may be interpreted as a slowing down of the 'rocking' process of the 'inside' 1,4-dioxybenzene ring between two different orientations within the tetracation, leading to the further observable splitting in the α-bipyridinium resonances ($\Delta\delta$ 0.15 ppm) and observed substantial broadening of the $-C_6H_4-$ and $^+NCH_2$ peaks at −85 °C. This process was found (Table 4) to have $k_c = 85$ s^{-1} at T_c of −65 °C in $(CD_3)_2CO$ ($\Delta\nu$ 38 Hz) with a $\Delta G_c^‡$ of 44 kJ mol^{-1}, which equates to around 9.3×10^4 reorientations per second of the 'inside' HQ ring at 25 °C.[29]

(ii) [2]catenanes from 3HQ porphyrins 11 and 12. Under similar reaction conditions to those used for the catenane formation of **14** from 2HQ porphyrins **6** and **7**, and using the equilibrated mixture of porphyrins containing three hydroquinone-derived rings (3HQ) **11a** and **12a**, a total of four catenated products was identified. NMR analysis indicated that these were formed in pairs in the same ratios (approximately 3:2) as the equilibrated mixture of starting porphyrins; they were subsequently identified as two [2]catenanes α,β-**15b** and α,α-**16b**, and two [3]catenanes α,β-**18b** and α,α-**17b** as shown in Scheme 3, in 21 and 6% overall yield, respectively.[30] Subsequent reactions on the isolated single isomers **11a** and **12a** indeed resulted in only two products in each case, the corresponding

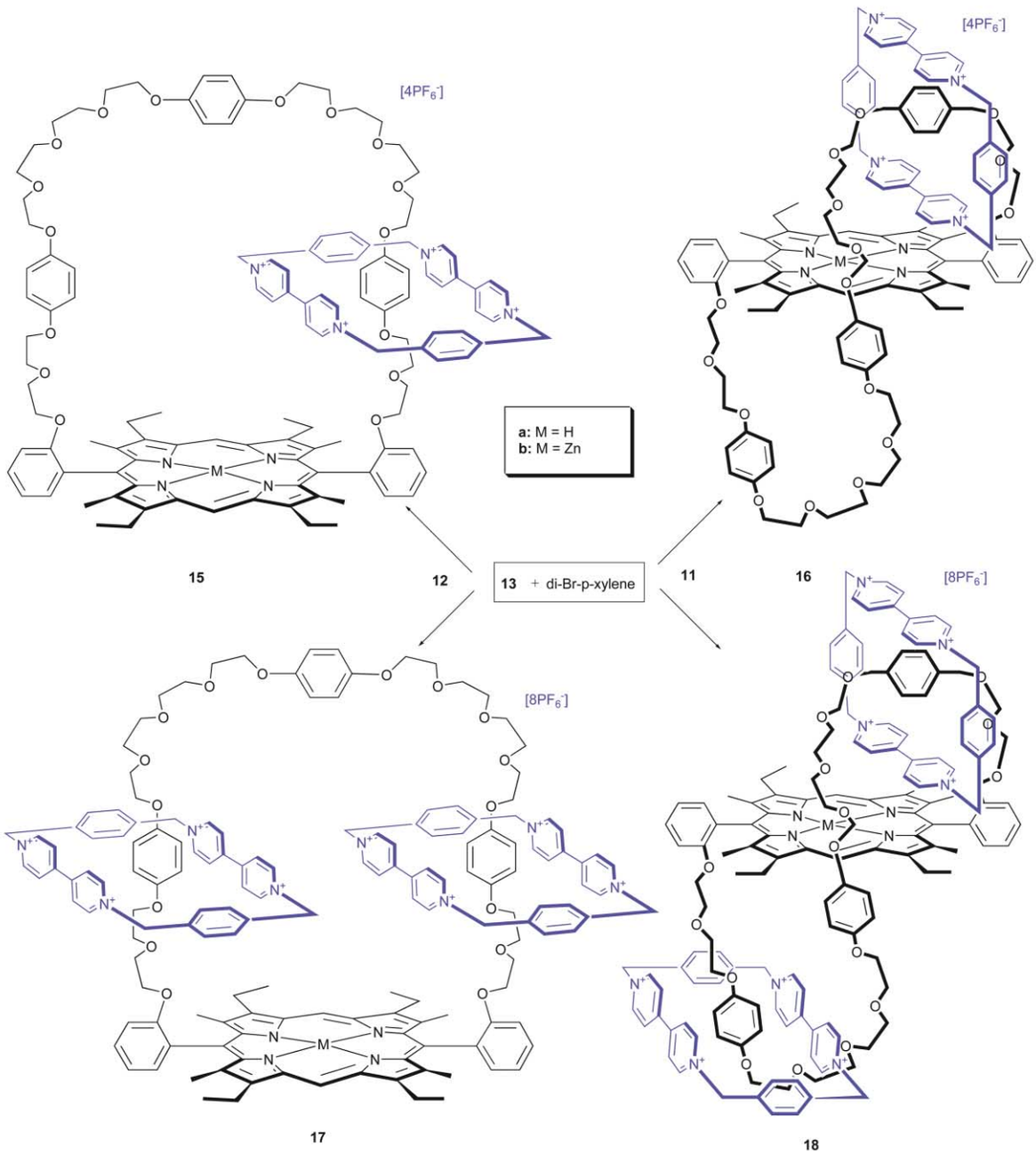

Scheme 3 Self-assembly of the isomeric strapped-porphyrin [2]catenanes **15** and **16**, and isomeric strapped-porphyrin [3]catenanes **17** and **18**, containing three hydroquinone-derived rings (3HQ). Reagents and conditions: DMF, 12 kbar, 6 days, then ZnOAc/MeOH/H_2O/acetone, followed by NH_4PF_6/H_2O.

atropisomeric [2] and [3]catenanes. Furthermore it was established that none of the isolated catenanes interconverted either under catenation conditions or subsequently during heating for several hours in refluxing acetonitrile.

FAB-MS of the individual isomers or mixtures of the 3HQ [2]catenanes (**16b** and **15b**) and [3]catenanes (**18b** and **17b**) were indicative of their proposed structures (Table 5). For the isomeric [2]catenanes (**16b** and **15b**), peaks corresponding to the successive loss of each counterion and the parent porphyrin ion peak were observed, as well as a small intensity peak corresponding to the parent catenane ion. For the isomeric [3]catenanes (**18b** and **17b**), peaks were observed for the successive loss of one to five PF_6^- counterions, as well as peaks corresponding to the loss of one tetracation together with successive loss of five to seven counterions. In addition, a peak corresponding to the parent porphyrin was also observed due to the unlinking of both tetracations and eight counterions, confirming the existence of the isomeric porphyrin [3]catenanes. Fig. 3 shows the spectrum of the [2]catenane **15b** compared to its corresponding starting porphyrin **12b**; the non-systematic numbering system used for proton assignments follows that in Scheme 1.

Catenation is indicated by a shielding (0.2ppm) of the *meso*-hydrogen compared to the starting porphyrin **12b**.[15] The resonances of the tetracationic moiety are shifted upfield compared to those of the original tetracation. Of significant interest are the shifts of the 1,4-dioxybenzene subunits (particularly positions H-21 and H-22 and H-21′ and H-22′ on the side of the strap) in the catenated compound **15b**, and particularly the fact that these show two distinct environments. The typical AB quartet resonances which are downfield (7.0 and 6.81 ppm respectively) are deshielded compared to those of the starting porphyrin **12b** and are assigned to H-21 and H-22. With the aid of gradient NOE experiments, the protons for the 1,4-dioxybenzene unit on the other side of the porphyrin (H-21′ and H-22′) were found at *ca.* 2.69 and 2.5 ppm which are

Table 5 Positive ion FAB mass spectrometry selected peaks for the catenanes **15b**, **16b**, **17b**, and **18b**

Peak	**15b**	**16b**	**17b**	**18b**
$[M]^+$	2613.1	2612.5	3712.6	3712.4
$[M–PF_6]^+$	2467.5	2468	3567.2	3567.7
$[M\text{-}2PF_6]^+$	2323	2323	3422.9	3423.2
$[M\text{-}3PF_6]^+$	2177.7	2177.9	3279.6	3279.3
$[M\text{-}4PF_6]^+$	—	—	3132.8	3133.3
$[M\text{-tetracation-}4PF_6]^+$	1511.2	1511.3	—	—
$[M\text{-}5PF_6]^+$	—	—	2987.8	2988.4
$[M\text{-tetracation-}5PF_6]^+$	—	—	2467.8	2467.5
$[M\text{-tetracation-}6PF_6]^+$	—	—	2323	2323
$[\text{Parent porphyrin}]^+$	1511.2	1511.3	1511.4	1511.7

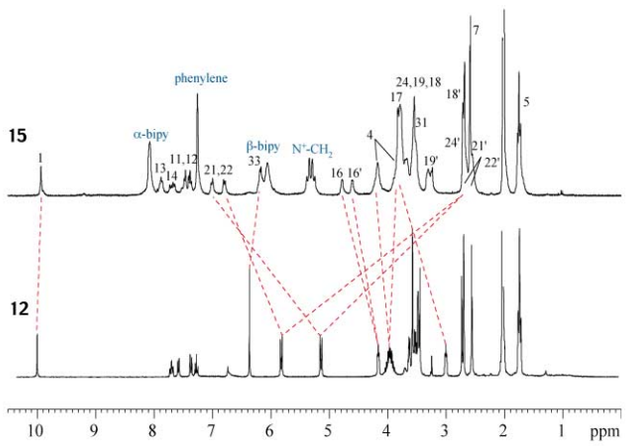

Fig. 3 ^{1}H NMR spectra of the porphyrin **12b** compared to its [2]catenane **15b** in acetone-d_6 at 303 K.

significantly shielded compared to those in **12b**. Thus, at 30 °C the tetracationic moiety is 'shuttling' between the two side 1,4-dioxybenzene units at a slow enough rate to observe the two environments on the NMR timescale at this frequency.

The downfield shifts for the 'unbound' protons H-21 and H-22 imply that this 1,4-dioxybenzene ring undergoes a change in conformation which reduces or counters the original shielding effect of the porphyrin in **12b** to allow π–π interactions between the bipyridinium moiety, the 'bound' 1,4-dioxybenzene unit (H-21′, H-22′) and the porphyrin, in a conformation as indicated in Fig. 4. The slow translational motion observed is further supported by the inequivalence of the ethylene glycol resonances H-16 to H-24, with H-16 having the smallest difference in shift. The largest chemical shift difference is seen for H-24 which indicates that the tetracationic macrocycle sits closer to the top side (over H-22′) of this 1,4-dioxybenzene unit. The central 1,4-dioxybenzene (B) unit is also shielded ($\Delta\delta$ 0.5 ppm), consistent with such a conformation. These results do not support an alternative structure in which the HQ-33 ring (ring B) is bound within the cavity of the tetracation and sandwiched between the two 'side' HQ rings (rings A), and held *orthogonal* to the porphyrin (structure **15′** in Fig. 4).

The broadness of the α- and β-bipyridinium resonances indicates that the tetracationic macrocycle is rotating as well as shuttling. At 30 °C this process is fast on the NMR time scale as there is no evidence for inside and outside environments for these resonances. The multiplicity of the N^+-methylene resonance is a commonly observed feature of related porphyrin catenanes, resulting from diastereotopicity of these protons.[15]

The ^{1}H NMR spectra of the twisted [2]catenane **16b** and its precusor porphyrin **11b** are shown in Fig. 5. Although the peaks are broadened at 30 °C, it was apparent from the exchange cross peaks that the 'shuttling' process observed for **15b** is also slow enough to be observed in this catenane at 30 °C. Interestingly, the 1,4-dioxybenzene protons H-33 do not shift on formation

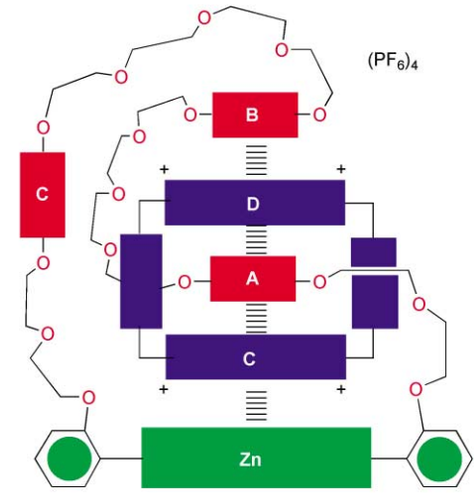

15

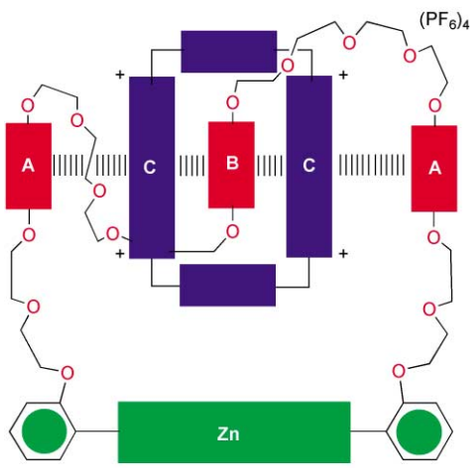

15'

Fig. 4 Conformation of [3]catenane **15** as deduced from NMR spectra; an alternative possible structure **15′**, in which the HQ-33 ring (ring B) is bound within the cavity of the tetracation and sandwiched between the two "side" HQ rings (rings A), and held *orthogonal* with the porphyrin, is not supported by the NMR evidence.

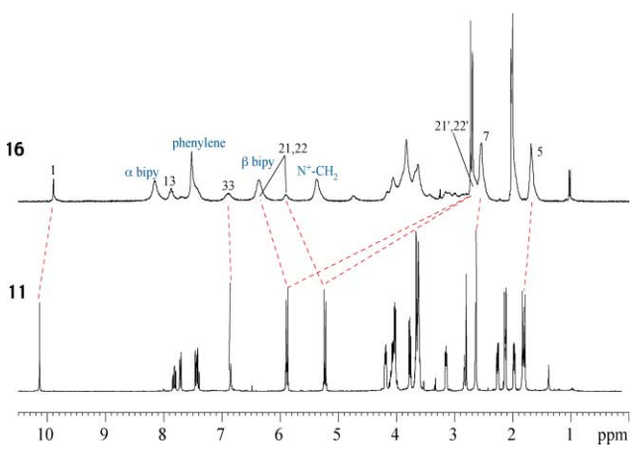

Fig. 5 ^{1}H NMR spectra of the porphyrin **11b** compared to its [2]catenane **16b** in acetone-d_6 at 303 K.

of the [2]catenane **16b**, indicating that this subunit's proximity to the edge of the porphyrin is little changed.

Dynamic NMR. At higher temperatures, both [2]catenanes undergo fast exchange in both the translational and rotational motions of the tetracationic macrocycle. Fig. 6 shows the

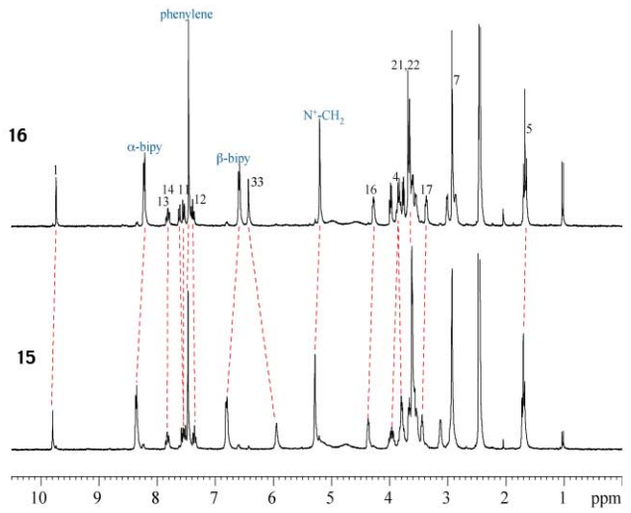

Fig. 6 ^{1}H NMR spectral comparison of the [2]catenanes **15b** and **16b** in DMSO-d_6 at 363 K.

comparative shifts of the protons for both **15b** and **16b**. It is apparent that at fast exchange, the difference in resonance shifts of both spectra have been greatly reduced, indicating similar rates of exchange (both translational and rotational) for both.

Nevertheless, the 1,4-dioxybenzene protons at position H-33 in **16b** are significantly deshielded ($\Delta\delta$ −0.49 ppm) compared to those of **15b**, accounting for their location at the edge of the porphyrin.

There are several dynamic processes observed in both of these [2]catenanes: (i) translational motion or 'shuttling' between the 1,4-dioxybenzene rings (A and C), with perhaps an intermediate 'stopover' on the central 1,4-dioxybenzene (B) subunit; (ii) tetracation rotation; and (iii) 'rocking' of the 1,4-dioxybenzene units. Because of this complexity, only the translational motion of the tetracationic macrocycle in compound **15b** between 1,4-dioxybenzene 'stations' (A) and (C) could be estimated by using the H-16,16′ protons and the coalescence method (Table 4). For **15b** a k of 2601 s^{-1} at T of 70 °C in CD_3CN ($\Delta\nu$ 828 Hz) with a $\Delta G^{\ddagger}$ of 62 kJ mol^{-1} was calculated, which equates to around 50 translations per second at 25 °C, and which is on par with the value determined by Stoddart for the translational motion for the BPP34C10-based [2]catenane **1b** of 120 s^{-1} with a $\Delta G^{\ddagger}_c$ of 65.3 kJ mol^{-1}. Likewise, evaluation of the peak separation observed in **16b** gave similar values, with k = 1926 s^{-1} at T of 70 °C in CD_3CN ($\Delta\nu$ 613 Hz) with a $\Delta G^{\ddagger}$ of 63 kJ mol^{-1}, which converts to around 35 translations per second at ambient temperature.

The rate is also about one order of magnitude faster than that calculated for the [2]catenane **14b**, indicating that the translational motion in the [2]catenane **15b** is less sterically restricted than in **14b**. In comparison to the Stoddart system **1b** however, it may reflect a stronger π–π interaction between the tetracation, bound 1,4-dioxybenzene ring and porphyrin moieties or a combination of all factors.

(iii) [3]catenanes from 3HQ porphyrins 11 and 12. The [3]catenane **18b** was also isolated from the reaction mixture of catenation of porphyrin isomer **16b**. When this was re-subjected to the catenation reaction conditions, no further change was observed, confirming that the porphyrin does not atropisomerise during the catenation reaction. Likewise, on prolonged heating above 90 °C in DMSO, no interconversion was observed, but some decomposition was evident at higher temperatures (>130 °C), resulting in the formation of an equilibrated mixture of the uncatenated porphyrins.

At 30 °C the spectrum was not as broad as observed in **16b**, and integration of the peaks for the bipyridinium macrocycle confirmed a [3]catenane. The diagnostic upfield shift of the *meso*-hydrogen ($\Delta\delta$ 0.2 ppm) also indicates catenation, and the sharpness of the peripheral ethyl H-7 and methyl protons H-5, and the ethylene glycol resonances, is indicative of higher symmetry in the structure compared to the [2]catenane **16b**.

Fig. 7 indicates a dynamic process expected for the [3]-catenane where the two macrocycles shuttle back and forth, exchanging between the 1,4-dioxybenzene units A and B. The macrocycles may move alternately or in tandem along the polyether chain. The upfield shift of the 1,4-dioxybenzene protons H-33 (B) into the region of δ 4.0–3.6 ppm is significant and indicates that this moiety is preferentially located 'inside' the macrocyclic cavity. This is also supported by the net deshielding effect observed for the α ($\Delta\delta$ 0.55 ppm) and β bipyridinium ($\Delta\delta$ 0.91 ppm) protons of the macrocycle compared to those in the [2]catenane **16b** because they, in turn, would experience more deshielding effects on average from the edge of the porphyrin subunit.

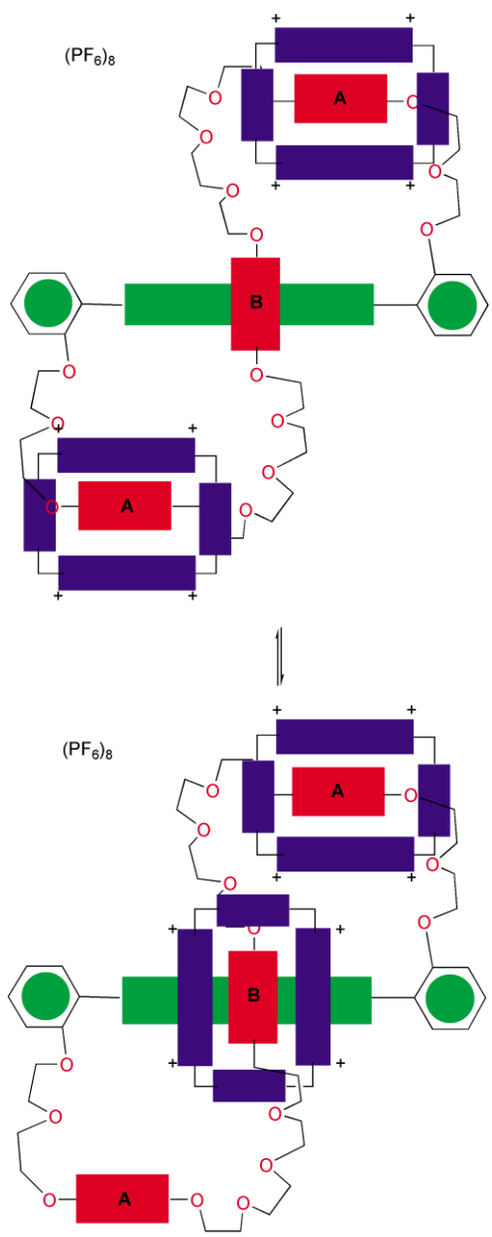

Fig. 7 Cartoon indicating the tandem or alternate shuttling which is possible in the [3]catenane **18**.

A clearer picture of the possible dynamics of **18b** can be gained by comparing it to the analogous [2]catenane **16b** at higher temperature (Fig. 8). The similarities of the ^{1}H NMR of **18b** and **16b** are quite obvious, although there are some important differences. Firstly, the α and β bipyridinium resonances

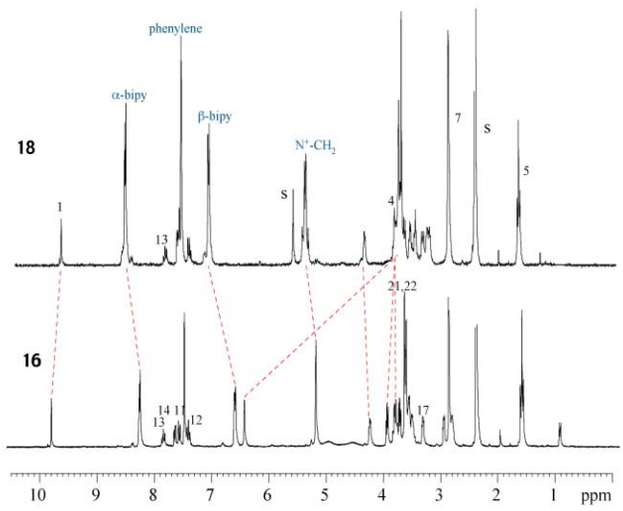

Fig. 8 ^{1}H NMR spectra of the [2]catenane **16b** compared to its [3]catenane counterpart **18b** at 363 K in DMSO-d_6.

are deshielded in the [3]catenane **18b** in comparison to the [2]catenane **16b** by 0.35 and 0.5 ppm, respectively. This can be attributed to the translational motion where there are now two charged macrocycles on the strap which means that these protons now have a longer time-averaged occupancy near the edge of the porphyrin encircling 1,4-dioxybenzene (B) and hence there is a net deshielding effect.[31]

Conversely, the 1,4-dioxybenzene protons H-33 are shielded ($\Delta\delta$ 0.8 ppm) which is as expected; the same translational motion of the two macrocycles also means that in fast exchange this subunit (B) would experience more time 'inside' one of the two charged cavities as demonstrated by Fig. 7. However, due to the presence of several processes (tetracation rotation, 'rocking' of the 1,4-dioxybenzene units and two possible modes of translational motion) and the broadness of the resonances at low temperatures, we were unable to evaluate exchange rates for this [3]catenane.[32]

Unfortunately, the second [3]catenane **17b** could not be isolated pure from the reaction mixture, and it was always contaminated with non-porphyrinic polymeric material. This, together with broadened ^{1}H NMR spectra, has prevented a full characterisation and evaluation of kinetic parameters. It was also clear that this catenane was less stable than its twisted isomer **18b**, and decomposition was observed when heated above 90 °C in DMSO solution, although no atropisomerisation to **18b** was observed. Mass and visible spectra were essentially identical to **18b**.

Nevertheless, it was clear that there are certain NMR spectral similarities and critical differences to the twisted isomer **18b**. At 30 °C in CD_3CN solution, broad resonances were observed corresponding to the HQ-33 (ring B) protons at δ 6.35 and 5.77 ppm for **17b**, compared to δ 6.94 and 6.86 ppm for the other isomer **18b**, indicating an exchange process which is slow on the NMR time scale at this temperature. The more upfield position (*ie* less deshielding of these protons in **17b** compared to **18b**) is consistent with the structures indicated, where the 'outside' HQ 33 would be deshielded in the twisted isomer **18b** compared to **17b**. On raising the temperature to 70 °C, these protons began to sharpen into one singlet in each case at δ 6.38 (**17b**) and 6.87 ppm (**18b**), although the resonance for **17b** was still somewhat broad. In addition, saturation transfer experiments at 70 °C revealed an 'inside' environment for these protons at δ 4.34 ppm (*cf*. 4.11 for **18b**), and this allowed an estimation of the translational motion, which was similar to that for the equivalent process in **18b**. It was also noticeable that the signals due to the methyl and ethyl groups on the porphyrin periphery were more symmetrical at lower temperatures than those of the twisted isomer **18b**.

Electronic spectra

UV-vis spectra of the 2HQ [2]catenane **14b** and 3HQ [2]catenanes (**16b** and **15b**) and [3]catenanes (**18b** and **17b**) showed the usual red shifts ($\Delta\lambda \sim 8$ nm) observed before in previous[15] porphyrin [2]catenanes. This indicates some form of electronic interaction between the porphyrin and tetracation subunits, despite the fact that any π–π charge transfer absorptions that may be present would be hidden under the large Soret absorption band of the porphyrin. However, the Soret and Q bands of the [3]catenane isomers were very broad with the usual Q band absorption at *ca*. 575 nm observed in all previous catenanes appearing as a very broad shoulder, clearly a direct effect of the second macrocycle.

Conclusions

A series of porphyrins strapped with polyether chains containing two or three 1,4-dioxybenzene units has been synthesised with a view to the production of porphyrin-containing [2] and [3]catenanes, where the porphyrin is strapped between *ortho*-positions of 5,15-(*meso*)-diaryl groups, and is interlinked with the bipyridinium macrocycle cyclo*bis*(paraquat-4,4′-biphenylene). The porphyrins were isolated as mixtures of atropisomers, where the linking strap spans across the face of the porphyrin (α,α-isomer), or 'twisted' around its side (α,β-isomer). Their structures have been determined by detailed ^{1}H NMR spectroscopy.

The *bis*-(1,4-dioxybenzene)-strapped derivatives have been shown to undergo atropisomerisation on heating, to produce an equilibrium mixture. Catenation under high pressure conditions of the mixture, or of the individual isomers, produced only a single catenane, that of the α,α-isomer. Its dynamics were measured, and rates were determined for (i) translational motion or 'shuttling' between 1,4-dioxybenzenes; (ii) 'rotation' of the macrocycle around the hydroquuinol axis; and (iii) 'rocking' of the 1,4-dioxybenzene within the macrocycle.

The atropisomers of the strapped derivatives containing *three* 1,4-dioxybenzene units were also separated, and subjected to catenation. Both [2]- and [3]catenanes have been isolated, and shown to be stable to further atropisomerisation. Their solution structures were probed in detail by dynamic ^{1}H NMR measurements. The rates for shuttling and rotation were obtained in certain cases, although the complexity of the spectra of the [3]catenanes precluded a more detailed investigation.

Thus we have demonstrated the viability of the synthesis of these porphyrin catenanes, in which the porphyrin subunit provides an ideal trigger for control of the dynamics, as it can be addressed by chemical, photochemical, or electrochemical stimuli. In this way, the assemblies can be regarded as molecular machines, in which mechanical motion can be controlled in a systematic and predictable manner. The way is now clear for the next generation of experiments.

Experimental

All solvents were distilled before use, using standard procedures: tetrahydrofuran (THF) was distilled over benzophenone and sodium under N_2; triethylamine (Et_3N) was distilled over CaH_2; dimethylformamide (DMF) was dried over type 4 Å molecular sieves. Column chromatography used Aldrich silica gel (grade 9385, 230–400 mesh). Preparative TLC was performed on 20 × 20 cm plates coated with 0.5 mm thick Art. 7731 Kieselgel 60 G Merck silica. Analytical TLC was carried out on Merck Silica Gel 60 G_{254} pre-coated aluminium sheets.

^{1}H NMR spectra were acquired using a 300 MHz Bruker Avance 300 spectrometer at 303 K, unless otherwise stated. Chemical shifts (δ) are reported in parts per million relative to residual solvent. Coupling constants (J) are reported in Hz.

Deuterated solvents were purchased from Aldrich and stored over type 3 Å molecular sieves after opening. COSY-45, gradient COSY, one-bond C–H correlation (HMQC), long-range C–H correlation (HMBC), NOESY, gradient NOESY two-dimensional NMR experiments employed the standard Bruker parameters. DEPT, NOE difference and saturation transfer experiments, as well selective gradient NOE experiments utilised standard Bruker pulse programs.

UV-Vis spectra were recorded on a Varian Cary IE UV-VIS spectrophotometer. Melting points were determined using a Reichert microscopic hot-stage apparatus.

FAB and ESI mass spectrometry was carried out by CSIRO Molecular Science at the Ian Wark Laboratory, Clayton and the Australian National University, Canberra, and high resolution ESI was performed at the Centre for Molecular Architecture, Rockhampton.

1,11-Bis{4-[2-(2-(toluene-*p*-sulfonyl)ethoxy)ethoxy]phenoxy}-3,6,9-trioxaundecane 3

1,11-Bis{4-[2-(2-hydroxyethoxy)ethoxy]-phenoxy}-3,6,9-trioxaundecane[7] 2 (4.64 g, 8.37 mmol) was dissolved with stirring in dry CH_2Cl_2 (40 mL) and Et_3N (2.12 g, 20.9 mmol). Then toluene-*p*-sulfonyl chloride (3.99 g, 20.9 mmol) and Et_3N (1.27 g, 12.6 mmol) in dry CH_2Cl_2 (40 mL), were added dropwise over 20 min, and the resulting solution was stirred at room temperature for 40 h. The solution was then poured into crushed ice and diluted with H_2O. The organic layer was separated, washed (2% HCl solution and H_2O), and dried ($MgSO_4$). Purification was carried out by column chromatography (silica) by eluting initially with CH_2Cl_2/petroleum spirit (1 : 1) and then (2 : 1) to remove impurities, followed by CH_2Cl_2 and then CH_2Cl_2/MeOH (1%) to obtain 3 as a yellow oil that solidified upon standing (5.79 g, 80%); δ_H (300 MHz; $CDCl_3$) 7.78 (4H, dd, *J* 8, 2, Ar–H), 7.29 (4H, d, *J* 8, Ar–H), 6.84–6.77 (8H, m, Ar–H), 4.18 (4H, t, *J* 5, OCH_2), 4.06 (4H, t, *J* 5, OCH_2), 3.97 (4H, t, *J* 5, OCH_2), 3.82 (4H, t, *J* 5, OCH_2), 3.75–3.66 (16H, m, OCH_2), 2.40 (6H, s, CH_3).

1,11-Bis{4-[2-(2-(*o*-formylphenoxy)ethoxy)ethoxy]phenoxy}-3,6,9-trioxaundecane 4

Salicylaldehyde (1.74 g, 1.43×10^{-2} mol) and K_2CO_3 (3.59 g, 2.60×10^{-2} mol) were stirred in dry CH_3CN (55 mL) with heating under an atmosphere of N_2 for 1 h. Then 1,4-dioxybenzene (2,4,2)-bistosylate **2** (5.6 g, 6.49 mmol) in dry CH_3CN (200 mL) was added all at once, and the resulting solution refluxed under N_2 for 4 days. Upon cooling, the reaction mixture was filtered, the solid washed (CH_2Cl_2), the solvent removed by rotary evaporation, and the residue partitioned between $CH_2Cl_2$and H_2O. The organic layer was separated, washed (H_2O), and dried ($MgSO_4$). The product was purified using column chromatography (silica) by eluting with CH_2Cl_2/petroleum spirit (1 : 1), (2 : 1), and then CH_2Cl_2 to remove impurities, followed by CH_2Cl_2/Et_2O (2%), increasing to CH_2Cl_2/Et_2O (10%) to afford **4** as a yellow oil that solidified upon standing. Recrystallised to obtain a white solid (4.11 g, 83%), mp 69–70 °C (from hot acetone with slow evaporation) (Found: C, 66.18; H, 6.48. $C_{42}H_{50}O_{13}$ requires C, 66.13; H, 6.61%); δ_H (300 MHz; $CDCl_3$) 10.51 (2H, s, CHO), 7.82 (2H, dd, *J* 8, 2, Ar–H), 7.52 (2H, dt, *J* 8, 2, Ar–H), 7.02 (2H, t, *J* 8, Ar–H), 6.98 (2H, d, *J* 8, Ar–H), 6.82 (8H, d, *J* 2, Ar–H), 4.26 (4H, t, *J* 5, OCH_2), 4.10–4.04 (8H, m, OCH_2), 3.97 (4H, t, *J* 5, OCH_2), 3.89 (4H, t, *J* 5, OCH_2), 3.81 (4H, t, *J* 5, OCH_2), 3.69 (8H, m, OCH_2).

Hydroquinone-derived (2,4,2)-porphyrin 6a and 7a

1,4-Dioxybenzene (2,4,2)-dialdehyde 4 (0.51 g, 6.69×10^{-4}mol) and 3,3′-diethyl-4,4′-dimethyl-2,2′-dipyrrylmethane (0.31 g, 1.34×10^{-3} mol) were dissolved with stirring in dry CH_3CN (70 mL). The solution was bubbled with $N_2$for 10 min, catalytic amounts of CCl_3COOH (*ca.* 60 mg) added, and the solution bubbled with N_2 again for 3 min. The reaction mixture was then stirred for 5 h (RT, N_2, dark), before adding *o*-chloranil (0.33 g, 1.34×10^{-3} mol) in THF (11 mL) all at once and stirring was continued overnight (RT, dark). Then added Et_3N (2 mL) and stirred for 30 min, before taking the solution to dryness by rotary evaporation. An initial purification was carried out on an alumina column using $CH_2Cl_2$and then CH_2Cl_2/Et_2O (2%) as the eluent to obtain several porphyrin fractions. Further purification was carried out by column chromatography (silica), eluting initially with CH_2Cl_2/Et_2O (2%) to remove impurities followed by CH_2Cl_2/Et_2O (5%) to obtain the porphyrin isomers **6a** and **7a**. A final purification on a fraction containing a mixture of **6a** and **7a** was carried out by preparative TLC plates using CH_2Cl_2/Et_2O (10%) as the eluent.

6a was recrystallised to obtain a purple/red solid (117 mg, 15%), mp 180–183 °C (from CH_2Cl_2/MeOH) (Found: C, 72.48; H, 7.21; N, 4.66. $C_{72}H_{84}N_4O_{11}.H_2O$ requires C, 72.09; H, 7.23; N, 4.67%); *m*/*z* (ESMS) $[M + H]^+$ 1182.1 (calcd. 1181.6), $[M + 2H]^{2+}$ 591.6 (calcd. 591.3); UV (λ nm, $CHCl_3$) 410, 507, 541, 574, 626; δ_H (300 MHz; $CDCl_3$, 298 K) 10.14 (2H, s, H-meso), 7.77 (2H, dd, *J* 7, 2,Ar–H), 7.74 (2H, dt, *J* 8, 2, Ar–H), 7.36 (2H, t, *J* 7, Ar–H), 7.29 (2H, d, *J* 8, Ar–H), 6.44 (4H, dd, *J* 7, 2, Ar–H), 5.94 (4H, dd, *J* 7, 2, Ar–H), 4.15 (4H, t, *J* 4, OCH_2), 4.01–3.84 (16H, m, CH_2CH_3(8H), OCH_2(8H)), 3.80 (8H, t, *J* 4, OCH_2), 3.20 (4H, t, *J* 4, OCH_2), 2.54 (12H, s, CH_3), 2.19 (8H, s, OCH_2), 1.70 (12H, t, *J* 8, CH_3CH_2), 1.26 (2H, s, H_2O), −2.36 (2H, br s, pyrrole NH).

7a was recrystallised to obtain a purple/red solid (55 mg, 7%), mp 184–186 °C (from CH_2Cl_2/MeOH) (Found: C, 71.85; H, 7.37; N, 4.43. $C_{72}H_{84}N_4O_{11}.H_2O$ requires C, 72.09; H, 7.23; N, 4.67%); *m*/*z* (ESMS) $[M + H]^+$ 1182.1 (calcd. 1181.6), $[M + 2H]^{2+}$ 591.6 (calcd. 591.3); UV (λ nm, $CHCl_3$) 410, 507, 542, 575, 626; δ_H (300 MHz; $CDCl_3$, 298 K) 10.17 (2H, s, H-meso), 7.79–7.74 (4H, m Ar–H), 7.35 (2H, t, *J* 7, Ar–H), 7.30 (2H, d, *J* 8, Ar–H), 6.37 (4H, d, *J* 9, Ar–H), 5.94 (4H, d, *J* 9, Ar–H), 4.16 (4H, t, *J* 4, OCH_2), 3.98 (8H, m, CH_2CH_3), 3.82 (4H, m, OCH_2), 3.70 (4H, m, OCH_2), 3.61 (8H, s, OCH_2), 3.12 (4H, t, *J* 4, OCH_2), 2.56 (12H, s, CH_3), 2.32 (4H, m, OCH_2), 2.23 (4H, m, OCH_2), 1.75 (12H, t, *J* 8, CH_3CH_2), 1.25 (2H, s, H_2O), −2.34 (2H, br s, pyrrole NH).

Zinc 1,4-dioxybenzene (2,4,2)-porphyrin 6b

Zinc was inserted into the 1,4-dioxybenzene (2,4,2)-porphyrin isomer **6a** to give **6b** which was recrystallised to obtain a purple/pink solid, mp 143–145 °C (from CH_2Cl_2/MeOH) (Found: C, 67.08; H, 6.30; N, 3.94. $C_{72}H_{82}N_4O_{11}.2H_2O$ requires C, 67.51; H, 6.77; N, 4.38%); UV (λ nm, $CHCl_3$) 412, 541, 576; δ_H (300 MHz; $CDCl_3$) 10.09 (2H, s, CHO), 7.74 (2H, d, *J* 8, Ar–H), 7.73 (2H, t, *J* 8, Ar–H), 7.35 (2H, t, *J* 7, Ar–H), 7.27 (2H, d, *J* 8, Ar–H), 6.52 (4H, dd, *J* 7, 2, Ar–H), 5.97 (4H, dd, *J* 7, 2, Ar–H), 4.12 (4H, t, *J* 4, OCH_2), 4.03 (4H, t, *J* 5, OCH_2), 3.94 (4H, m, CH_2CH_3), 3.85 (8H, m, CH_2CH_3 (4H), OCH_2 (4H)), 3.79 (8H, t, *J* 5, OCH_2), 3.17 (4H, t, *J* 4, OCH_2), 2.51 (12H, s, CH_3), 2.21 (4H, m, OCH_2), 2.10 (4H, m, OCH_2), 1.69 (12H, t, *J* 8, CH_3CH_2), 1.24 (4H, s, $2H_2O$).

Zinc 1,4-dioxybenzene (2,4,2)-porphyrin 7b

Zinc was inserted into the 1,4-dioxybenzene (2,4,2)-porphyrin **7a** to give **7b**, which was recrystallised to obtain a purple/pink solid, mp 176–180 °C (from CH_2Cl_2/MeOH) (Found: C, 68.73; H, 6.66; N, 4.17. $C_{72}H_{82}N_4O_{11}.H_2O$ requires C, 68.48; H, 6.70; N, 4.44%); UV (λ nm, $CHCl_3$) 412, 540, 575; δ_H (300 MHz; $CDCl_3$) 10.15 (2H, s, meso-H), 7.80 (2H, d, *J* 8, Ar–H), 7.79 (2H, t, *J* 8, Ar–H), 7.39 (2H, t, *J* 8, Ar–H), 7.32 (2H, d, *J* 9, Ar–H), 6.44 (4H, d, *J* 9, Ar–H), 5.98 (4H, d, *J* 9, Ar–H), 4.17 (4H, t, *J* 4, OCH_2), 4.03–3.98 (8H, m, CH_2CH_3), 3.86 (4H, t, *J* 4, OCH_2), 3.71 (4H, m, OCH_2), 3.60 (8H, s, OCH_2), 3.15 (4H,

t, *J* 4, OCH_2), 2.57 (12H, s, CH_3), 2.36 (4H, m, OCH_2), 2.20 (4H, m, OCH_2), 1.78 (12H, t, *J* 8, CH_3CH_2).

Catenane 14b

Zinc 1,4-dioxybenzene (2,4,2) porphyrin isomers [**6b** (*ca*. 20%) and **7b** (*ca*. 80%), estimated from NMR] (110 mg, 8.84×10^{-5} mol), 1,1′-[1,4-phenylenebis(methylene)]bis(4,4′-bipyridinium)-bis-(hexafluorophosphate) **13**[27] (187 mg, 2.65×10^{-4} mol), 1,4-bis(bromomethyl)benzene (87 mg, 3.31×10^{-4} mol), and catalytic amounts of NaI and NH_4PF_6 were dissolved in DMF (7 mL), deoxygenated with N_2 for 20 min, and then stirred at room temperature at 12 Kbar for 3 days. The reaction mixture was then filtered and the solvent removed under vacuum with heating. The combined solid residues were then washed well with CH_2Cl_2, followed by hot H_2O. Purification was carried out by column chromatography (silica) by eluting initially with CH_2Cl_2/MeOH (10%) then MeOH, followed by MeOH/2M NH_4Cl solution/$MeNO_2$ (7 : 2 : 1 v/v). The product fractions were taken to dryness, the residue dissolved in a minimum amount of MeOH/H_2O/acetone, and a solution of $Zn(OAc)_2$ in MeOH was added and allowed to stir at room temperature for 3 h. The acetone was then removed, the solution filtered, the solid dissolved in a minimum amount of MeOH/H_2O/acetone, and the product taken to dryness again. The residue was then dissolved in a minimum amount of MeOH/H_2O, and saturated NH_4PF_6 solution added until no further precipitation was evident. The catenane product was collected by filtration, washed (H_2O), and pumped dry. The solid was then washed with acetone and the filtrate recrystallised to obtain **14b** as a dark purple solid (82 mg, 40%), mp 223–225 °C (from acetone/$^iPr_2O$) (Found: C, 54.24; H, 4.75; N, 4.58. $C_{108}H_{114}N_8O_{11}$-$Zn(PF_6)_4 \cdot 2H_2O$ requires C, 54.46; H, 4.99; N, 4.71%); *m*/*z* (ESMS) $[M + H - PF_6]^+$ 2198.7 (calcd. 2198.7), $[M + H -$ tetracation $- 4PF_6]^+$1243.2 (calcd. 1243.5), $[M - 2PF_6]^{2+}$ 1026.8 (calcd. 1026.4), $[M - 3PF_6]^{3+}$636.2 (calcd. 635.9), $[M -$ tetracation $- 4PF_6]^{2+}$621.4 (calcd. 621.3), $[M + 4H]^{4+}$587.1 (calcd. 586.7), $[M - 4PF_6]^{4+}$ 440.7 (calcd. 440.7); UV (λ nm, acetone) 421, 540, 574; δ_H (300 MHz; acetone) 10.03 (2H, s, H-meso), 8.29 (8H, br s, α-bipy), 7.90 (2H, m, Ar–H), 7.69 (3H, m, Ar–H), 7.46 (1H, t, *J* 6, Ar–H), 7.39 (2H, m, Ar–H), 7.06 (8H, s, $-C_6H_4-$), 6.73 (10H, m, β-bipy (8H), Ar–H (2H)), 6.56 (2H, d, J 9, Ar–H), 5.31 (4H, d, *J* 13, $^+N-CH_2$), 4.98 (4H, d, *J* 13, $^+N-CH_2$), 4.77 (2H, s, OCH_2), 4.63 (2H, s, OCH_2), 4.17 (4H, m, CH_2CH_3), 4.06 (4H, m, CH_2CH_3), 4.00 (2H, s, OCH_2), 3.95 (2H, s, OCH_2), 3.86–3.81 (6H, m, OCH_2), 3.74 (8H, s, OCH_2), 3.66 (4H, s, OCH_2), 3.22 (2H, s, OCH_2), 3.11 (2H, s, OCH_2), 3.02 (2H, d, *J* 9, Ar–H), 2.85 (2H, m, OCH_2), 2.71 (2H, m, Ar–H), 2.67 (6H, s, CH_3), 2.59 (6H, s, CH_3), 1.80 (12H, m, CH_3CH_2); δ_H (300 MHz; CD_3CN) 9.90 (2H, s, H-meso), 7.93 (2H, m, Ar-H), 7.71 (8H, d, *J* 4, α-bipy), 7.68 (3H, m, Ar–H), 7.45 (1H, t, J 6, Ar–H), 7.38 (2H, m, Ar–H), 7.10 (8H, s, $-C_6H_4-$), 6.91 (2H, d, J 8, Ar–H), 6.68 (2H, d, J 9, Ar–H), 5.99 (8H, d, *J* 4, β-bipy), 5.03 (4H, d, *J* 13, $^+N-CH_2$), 4.77 (4H, d, *J* 13, $^+N-CH_2$), 4.61 (2H, s, OCH_2), 4.53 (2H, s, OCH_2), 4.21 (4H, m, CH_2CH_3), 4.05 (2H, s, OCH_2), 3.94–3.84 (12H, m, CH_2CH_3 (4H), OCH_2 (8H)), 3.75–3.72 (4H, m, OCH_2), 3.63 (4H, s, OCH_2), 3.53 (4H, m, OCH_2), 3.04 (2H, s, OCH_2), 2.92 (2H, s, OCH_2), 2.71 (2H, s, OCH_2), 2.69 (2H, m, Ar–H), 2.63 (6H, s, CH_3), 2.56 (6H, s, CH_3), 2.36 (2H, d, J 7, Ar–H), 1.80 (12H, m, CH_3CH_2).

The above reaction was also performed with equilibrium mixtures of **6b** and **7b** (158 mg, 1.27×10^{-4} mol), and 2.5 mole equivalents less of **13** (107 mg, 1.52×10^{-4} mol) and 1,4-bis-(bromomethyl)benzene (50 mg, 1.91×10^{-4} mol), as well as catalytic amounts of NaI and NH_4PF_6 using the same reaction conditions and workup procedure to that above, gave **14b** (58 mg, 20%).

Reaction with equilibrium mixtures of **6b** and **7b** (230 mg, 1.95×10^{-4} mol), **13** (165 mg, 2.34×10^{-4} mol) and 1,4-bis-(bromomethyl)benzene (77 mg, 2.93×10^{-4} mol), as well as catalytic amounts of NaI and NH_4PF_6 with stirring at ambient temperature and pressure for 17 days in DMF (6 mL), was also carried out using the same workup procedure to that above to give **14b** (3.5 mg, 1%).

1,4-Bis{2-{2-{2-{2-{[2-(2-(toluene-*p*-sulfonyl)ethoxy)ethoxy]-phenoxy}ethoxy}-ethoxy}ethoxy}ethoxy}benzene 9

1,4-Bis{2-{2-{2-{2-{[2-(2-hydroxyethoxy)ethoxy]phenoxy}-ethoxy}ethoxy}ethoxy}ethoxy}benzene **8**[7] (5.91 g, 7.18 mmol) was dissolved with stirring in dry CH_2Cl_2 (50 mL) and Et_3N (1.82 g, 18.0 mmol). Then toluene-*p*-sulfonyl chloride (3.42 g, 18.0 mmol) and Et_3N (1.09 g, 10.8 mmol) in dry CH_2Cl_2 (50 mL), were added dropwise over 30 min, a drying tube connected, and the resulting solution stirred for 36 h at room temperature. The reaction mixture was then poured into crushed ice and diluted with H_2O. The organic layer was separated, washed (2% HCl solution and H_2O), and dried (Na_2SO_4). Purification was carried out by column chromatography (silica) by eluting initially with CH_2Cl_2/petroleum spirit (1 : 1) and then CH_2Cl_2 to remove impurities, followed by CH_2Cl_2/Et_2O (20%) to obtain **9** as a yellow oil, which was recrystallised to form a white solid (4.71 g, 58%), mp 81–83 °C (from cold acetone) (Found: C, 59.02; H, 6.70. $C_{56}H_{74}O_{20}S_2$ requires C, 59.45; H, 6.59%); δ_H (300 MHz; $CDCl_3$) 7.77 (4H, dd, *J* 7, 2, Ar–H), 7.28 (4H, d, *J* 8, Ar–H), 6.80 (8H, s, Ar–H), 6.79 (4H, s, Ar–H), 4.17 (4H, t, *J* 5, OCH_2), 4.04 (8H, m, OCH_2), 3.96 (4H, t, *J* 5, OCH_2), 3.80 (8H, dt, *J* 5, 2, OCH_2), 3.74–3.67 (24H, m, OCH_2), 2.39 (6H, s, CH_3).

1,4-Bis{2-{2-{2-{2-{[2-(2-(*o*-formylphenoxy)ethoxy)ethoxy]-phenoxy}ethoxy}ethoxy}-ethoxy}ethoxy}benzene 10

Salicylaldehyde (1.07 g, 8.73 mmol) and K_2CO_3 (2.74 g, 1.98×10^{-2} mol) were stirred in dry CH_3CN (50 mL) with heating under an atmosphere of N_2 for 20 min. Then 1,4-dioxybenzene (2,4,4,2)-bistosylate **9** (4.49 g, 3.97 mmol) in dry CH_3CN (130 mL) was added all at once, and the resulting solution refluxed under N_2 for 60 h. Upon cooling, the reaction mixture was filtered, the solid washed ($CHCl_3$), the solvent removed by rotary evaporation, and the residue partitioned between $CHCl_3$and H_2O. The organic layer was separated, washed (2M NaOH solution, H_2O), and dried (Na_2SO_4). Purification was carried out by multiple fractional recrystallisations to obtain **10** as a white solid (1.38 g, 33%), mp 79–80 °C (from CH_2Cl_2/MeOH with slow evaporation) (Found: C, 64.87; H, 6.64. $C_{56}H_{70}O_{18}$ requires C, 65.23; H, 6.84%); δ_H (300 MHz; $CDCl_3$) 10.49 (2H, s, CHO), 7.80 (2H, d, *J* 9, Ar–H), 7.50 (2H, t, *J* 8, Ar–H), 7.01 (2H, t, *J* 8, Ar–H), 6.96 (2H, d, *J* 9, Ar–H), 6.80 (12H, d, *J* 3, Ar–H), 4.25 (4H, t, *J* 4, OCH_2), 4.08–4.03 (12H, m, OCH_2), 3.95 (4H, t, *J* 4, OCH_2), 3.88 (4H, t, *J* 4, OCH_2), 3.79 (8H, t, *J* 4, OCH_2), 3.68 (16H, m, OCH_2).

1,4-dioxybenzene (2,4,4,2)-porphyrin 11a and 12a

1,4-dioxybenzene (2,4,4,2)-dialdehyde **10** (0.24 g, 2.25×10^{-4} mol) and 3,3′-diethyl-4,4′-dimethyl-2,2′-dipyrrylmethane **5** (0.11 g, 4.50×10^{-4} mol) were dissolved with stirring in dry CH_3CN (20 mL), and the solution bubbled with N_2 for 20 min. Then Cs_2CO_3 (90 mg, 2.70×10^{-4} mol) and CCl_3COOH (90 mg, 5.40×10^{-4} mol) in dry CH_3CN (5 mL), together with additional catalytic amounts of CCl_3COOH were added all at once, and the solution bubbled with N_2 again for 3 min. The reaction mixture was then stirred for 5 h (RT, N_2, dark), before adding *o*-chloranil (0.11 g, 4.50×10^{-4} mol) in dry THF (5 mL) all at once and stirring was continued overnight (RT, dark). Then Et_3N (1 mL) was added and the mixture was stirred for 30 min, before taking the solution to dryness by rotary evaporation. An initial purification was carried out on an alumina column using CH_2Cl_2/MeOH (5%) as the eluent to obtain several porphyrin

fractions. Further purification was carried out by column chromatography (silica), eluting with CH_2Cl_2/Et_2O (30%) to obtain the porphyrin isomer **11a** and with CH_2Cl_2/Et_2O (40%) to obtain the porphyrin isomer **12a**. A final purification on both fractions was carried out by preparative TLC plates using CH_2Cl_2/Et_2O (20%) as the eluent.

11a was recrystallised to obtain a purple/red solid (45 mg, 14%), m.p. 155–158 °C (from CH_2Cl_2/MeOH) (Found: C, 69.66; H, 7.03; N, 3.80. $C_{86}H_{104}O_{16}N_4.2H_2O$ requires C, 69.52; H, 7.33; N, 3.77%); *m/z* (ESMS) $[M + H]^+$ 1450.4 (calcd. 1449.7), $[M + 2H]^{2+}$ 725.7 (calcd. 725.4); UV (λ nm, $CHCl_3$) 410, 507, 541, 574, 626; δ_H (300 MHz; $CDCl_3$) 10.20 (2H, s, H-meso), 7.83–7.77 (4H, m, Ar–H), 7.40 (2H, t, *J* 8, Ar–H), 7.34 (2H, d, *J* 9, Ar–H), 6.89 (4H, s, Ar–H), 5.86 (4H, d, *J* 9, Ar–H), 5.20 (4H, d, *J* 9, Ar–H), 4.17 (4H, t, *J* 4, OCH_2), 4.10 (4H, t, *J* 4, OCH_2), 4.00 (8H, m, CH_2CH_3), 3.87 (4H, t, *J* 4, OCH_2), 3.75–3.66 (24H, m, OCH_2), 3.20 (4H, t, *J* 4, OCH_2), 2.59 (12H, s, CH_3), 2.06 (4H, t, *J* 4, OCH_2), 1.77 (12H, t, *J* 8, CH_3CH_2), 1.63 (4H, t, *J* 4, OCH_2), 1.28 (4H, s, $2H_2O$), −2.27 (2H, br s, pyrrole NH).

12a was recrystallised to obtain a purple/red solid (12 mg, 4%), mp 142–145 °C (from CH_2Cl_2/MeOH) (Found: C, 69.98; H, 6.93; N, 3.85. $C_{86}H_{104}O_{16}N_4.H_2O$ requires C, 70.37; H, 7.28; N, 3.82%); *m/z* (ESMS) $[M + H]^+$ 1450.4 (calcd. 1449.7), $[M + 2H]^{2+}$ 725.7 (calcd. 725.4); UV (λ nm, $CHCl_3$) 410, 507, 541, 573, 626; δ_H (300 MHz; $CDCl_3$) 10.21 (2H, s, H-meso), 7.82–7.77 (4H, m, Ar–H), 7.39 (2H, t, *J* 8, Ar–H), 7.32 (2H, d, *J* 9, Ar–H), 6.54 (4H, s, Ar–H), 5.84 (4H, d, *J* 9, Ar–H), 5.24 (4H, d, *J* 9, Ar–H), 4.18 (4H, t, *J* 4, OCH_2), 4.01 (8H, m, CH_2CH_3), 3.80 (4H, t, *J* 4, OCH_2), 3.70 (8H, m, OCH_2), 3.62 (20H, m, OCH_2), 3.10 (4H, t, *J* 4, OCH_2), 2.60 (12H, s, CH_3), 2.07 (4H, t, *J* 4, OCH_2), 1.79 (12H, t, *J* 8, CH_3CH_2), 1.72 (4H, t, *J* 4, OCH_2), 1.28 (2H, s, H_2O), −2.25 (2H, br s, pyrrole NH); δ_C ($CDCl_3$) 158.6, 152.9, 152.1, 152.0, 145.4, 144.4, 140.9, 135.8, 134.5, 131.3, 130.3, 121.1, 115.4, 114.6, 114.2, 111.8, 96.1, 70.9, 70.8, 69.8, 69.3, 68.7, 67.9, 67.7, 65.6, 19.9, 17.7 and 13.7.

Zinc 1,4-dioxybenzene(2,4,4,2)porphyrin 12b

Zinc was inserted into the 1,4-dioxybenzene (2,4,4,2) porphyrin H_2(3HQ)2,4,4,2P **12a** to give **12b**, which was recrystallised to obtain a purple/pink solid, mp 73–77 °C (from CH_2Cl_2/heptane); UV (λ nm, $CHCl_3$) 412, 540, 575; δ_H (300 MHz; $CDCl_3$) 10.16 (2H, s, H-meso), 7.80 (4H, m, Ar–H), 7.39 (2H, t, *J* 8, Ar–H), 7.34 (2H, d, *J* 7, Ar–H), 6.60 (4H, s, Ar–H), 6.06 (4H, d, *J* 9, Ar–H), 5.48 (4H, d, *J* 9, Ar–H), 4.18 (4H, t, *J* 4, OCH_2), 4.02 (8H, m, CH_2CH_3), 3.82 (4H, t, *J* 4, OCH_2), 3.68 (12H, m, OCH_2), 3.60 (16H, m, OCH_2), 3.11 (4H, t, *J* 4, OCH_2), 2.58 (12H, s, CH_3), 2.15 (4H, t, *J* 4, OCH_2), 2.03 (4H, m, OCH_2), 1.78 (12H, t, *J* 8, CH_3CH_2).

Catenanes 15, 16, 17 and 18

[2]catenane 16b and [3]catenane 18b. The free base 1,4-dioxybenzene (2,4,4,2) α,β-porphyrin (161 mg, 1.11×10^{-1} mmol) 1,1′-[1,4-phenylenebis(methylene)]bis(4,4′-bipyridinium)bis-(hexa-fluorophosphate) **13** (330 mg, 4.67×10^{-1} mmol), 1,4-bis(bromomethyl)benzene (150 mg, 5.83×10^{-1} mmol), and catalytic amounts of NaI and NH_4PF_6 were dissolved in DMF (7 mL), then stirred at room temperature at 12 kbar for 6 days. The solvent was removed under vacuum with heating, and the residue washed well with CH_2Cl_2, followed by hot water. Purification was carried out by column chromatography (silica) by eluting initially with CH_2Cl_2/MeOH (10%), then MeOH/2M NH_4Cl solution/$MeNO_2$ (7:2:1 v/v) to obtain the [2]-catenane fraction **16a**, followed by MeOH/2M NH_4Cl solution/DMF (4:5:2 v/v) to obtain the [3]-catenane **18a**. The [2]-catenane fraction was taken to dryness, the residue dissolved in a minimum amount of MeOH/water/acetone, and a solution of $Zn(OAc)_2$ in MeOH was added and allowed to stir at room temperature for 1 h. The acetone was then removed, the solution filtered, and saturated NH_4PF_6 solution added to the filtrate until no further precipitation was evident. The [2]-catenane product was collected by filtration, washed (water), and pumped dry. The solid was then washed with acetone and the filtrate recrystallised (from acetone/^{i}Pr$_2$O) to obtain the porphyrin [2]-catenane **16b** as a dark purple solid (39 mg, 21%), mp 200–204 °C; *m/z* (FAB) $[M]^+$ 2612.0 (calcd 2612.79), $[M–PF_6]^+$ 2467.0 (calcd 2467.83), $[M\text{-}2PF_6]^+$ 2322.0 (calcd 2322.86), $[M\text{-}3PF_6]^+$ 2177.0 (calcd 2177.90), [M-tetracation-PF_6]$^+$ 1511.3 (calcd 1512.67); δ_H (300 MHz; DMSO-d_6; 363K) 9.74 (2H, s, H-1), 8.22 (8H, d, *J* 6, α-bipy), 7.82 (2H, t, *J* 9, H-13), 7.62 (2H, d, *J* 8, H-14), 7.55 (2H, d, *J* 8, H-11), 7.46 (8H, s, phenylene), 7.39 (2H, t, *J* 8, 12), 6.59 (8H, d, *J* 6, β-bipy), 6.43 (4H, s, H-33), 5.21 (8H, s, $N^+–CH_2$), 4.28 (4H, m, H-16), 3.99 (4H, m, OCH_2), 3.84 (8H, m, H-4), 3.67–3.62 (24H, m, H-21, H-22, 4 × OCH_2), 3.61 (4H, m, OCH_2), 3.57 (4H, m, OCH_2), 3.37 (4H, m, H-17), 3.00 (4H, m, OCH_2), 2.93 (16H, s, H-7, OCH_2), 2.88 (4H, m, OCH_2), 1.68 (12H, t, *J* 8, H-5).

18b was also collected and recrystallised in the same manner (15 mg, 6%), mp 234–237 °C; *m/z* (FAB)- $[M]^+$ 3712.4 (calcd 3712.91), $[M–PF_6]^+$ 3567.7 (calcd 3567.95), $[M\text{-}2PF_6]^+$ 3423.2 (calcd 3422.98), $[M\text{-}3PF_6]^+$ 3279.3 (calcd 3278.02), $[M\text{-}4PF_6]^+$ 3133.3 (calcd 3133.06), $[M\text{-}5PF_6]^+$ 2988.4 (calcd 2988.09), [M-tetracation-$5PF_6$]$^+$ 2467.5 (calcd 2467.83), [M-tetracation-$5PF_6$]$^+$ 2323 (calcd 2322.86), [parent porphyrin]$^+$ 1511.7 (calcd 1512.67); δ_H (300 MHz; DMSO-d_6; 363 K) 9.70 (2H, s, H-1), 8.58 (16H, d, *J* 6, α-bipy), 7.87 (2H, t, J 9, H-13), 7.67–7.63 (4H, m, H-14, H-11), 7.60 (16H, s, phenylene), 7.46 (2H, t, *J* 8, H-12), 7.12 (16H, d, *J* 6, β-bipy), 5.45 (16H, m, $N^+–CH_2$), 4.40 (4H, m, H-16), 3.87 (8H, m, H-4), 3.80–3.68 (28H, m, H-21, H-22, H-33, 4 × OCH_2), 3.60 (4H, m, OCH_2), 3.51 (4H, m, H-17), 3.40 (4H, m, OCH_2), 3.31–3.26 (8H, m, OCH_2), 2.93 (20H, s, H-7, OCH_2), 1.70 (12H, t, *J* 8, H-5).

[2] catenane 15b and [3]catenane 17b. The free base 1,4-dioxybenzene (2,4,4,2) α,α-porphyrin **12a** (183 mg, 1.26×10^{-4}mol) 1,1′-[1,4-phenylenebis(methylene)]bis(4,4′-bipyridinium)bis-(hexafluorophosphate)[27] **13** (370 mg, 5.30×10^{-4}mol), 1,4-bis(bromomethyl)benzene (170 mg, 6.62×10^{-4}mol), and catalytic amounts of NaI and NH_4PF_6 were dissolved in DMF (7 mL), then stirred at room temperature at 12 kbar for 6 days. The solvent was removed under vacuum with heating, and the residue washed well with CH_2Cl_2, followed by hot water. Purification was carried out by column chromatography (silica) by eluting initially with CH_2Cl_2/MeOH (10%), then MeOH/2M NH_4Cl solution/$MeNO_2$ (7:2:1 v/v) to obtain the [2]-catenane fraction **15b**, followed by MeOH/2M NH_4Cl solution/DMF (4:5:2 v/v) to obtain the [3]-catenane **17b**. The [2]-catenane fraction was taken to dryness, the residue dissolved in a minimum amount of MeOH/water/acetone, and a solution of $Zn(OAc)_2$ in MeOH was added and allowed to stir at room temperature for 1 h. The acetone was then removed, the solution filtered, and saturated NH_4PF_6 solution added to the filtrate until no further precipitation was evident. The product was collected by filtration, washed (water), and pumped dry. The solid was then washed with acetone and the filtrate recrystallised to obtain the porphyrin [2]catenane **15b** as a dark purple solid (24 mg 13%), mp 200–204 °C (from acetone/^{i}Pr$_2$O); *m/z* (FAB) $[M]^+$ 2612.0 (calcd 2612.79), $[M–PF_6]^+$ 2467.5 (calcd 2467.83), $[M\text{-}2PF_6]^+$ 2323.0 (calcd 2322.86), $[M\text{-}3PF_6]^+$ 2177.0 (calcd 2177.90), [M-tetracation-$4PF_6$]$^+$ 1511.7 (calcd 1512.67); δ_H (300 MHz; CD_3COCD_3; 300 K) 9.94 (2H, s, H-1), 8.08 (8H, d, *J* 6, α-bipy), 7.89 (2H, t, *J* 9, H-13), 7.72–7.65 (2H, d, *J* 8, H-14, H-14′), 7.46 (2H, d, *J* 8, H-11), 7.41 (2H, t, *J* 8, H-12), 7.26 (8H, s, phenylene), 7.00 (2H, d, *J* 8, H-21), 6.81 (2H, d, *J* 8, H-22), 6.17 (4H, d, *J* 8, H-33), 6.06 (8H, bs, β-bipy), 5.32 (8H, m, $N^+–CH_2$), 4.79 (2H, m, H-16), 4.61 (2H, m, H-16′), 4.17 (4H, m, H-4), 3.82–3.45 (24H, m, H-4′, H-17, H-24, H-19, H-18, H-31, 2 × OCH_2), 3.29 (6H, m, H-19′, OCH_2), 2.71 (12H, m, H-24′, H-18′, 2 × OCH_2), 2.59 (16H, bs, H-7, H-21′, H-22′),

1.76 (12H, t, *J* 8, H-5); δ_H (300 MHz; DMSO-d_6; 363 K) 9.80 (2H, s, H-1), 8.36 (8H, d, *J* 6, α-bipy), 7.83 (2H, t, *J* 9, H-13), 7.57 (2H, d, *J* 8, H-14), 7.54 (2H, d, *J* 8, H-11), 7.51 (8H, s, phenylene), 7.36 (2H, t, *J* 8, H-12), 6.80 (8H, d, *J* 6, β-bipy), 5.95 (4H, s, H-33), 5.29 (8H, s, N^+–CH_2), 4.37 (4H, m, H-16), 3.97 (4H, m, H-4), 3.80 (8H, m, H-4, OCH_2), 3.68–3.55 (32H, m, H-21, H-22, 6 × OCH_2), 3.45 (4H, m, H-17), 3.13 (4H, m, OCH_2), 2.93 (20H, s, H-7, 2 × OCH_2), 1.71 (12H, t, *J* 8, H-5).

Catenane **17b** was obtained similarly (10 mg, 5%). NMR analysis indicated very broad peaks, and that this fraction was contaminated with polymeric bipyridinium-based material, which could not be separated. Nevertheless, certain peaks belonging to the catenane could be assigned, as their ratio did not vary after each attempted purification step; *m*/*z* (FAB) $[M\text{-}PF_6^-]^+$ 3566.8 (calcd 3565.9), $[M\text{-}2PF_6]^+$ 3421.7 (calcd 3421.0), $[M\text{-}3PF_6]^+$ 3276.8 (calcd 3276.0), $[M\text{-}4PF_6]^+$ 3131.9 (calcd 3131.0), $[M\text{-}5PF_6]^+$ 2986.9 (calcd 2986.1), [M-tetracation-$5PF_6$]$^+$ 2465.9 (calcd 2465.8), [M-tetracation-$6PF_6$]$^+$ 2320.9 (calcd 2320.8), [M-tetracation-$7PF_6$]$^+$, [M-2(tetracation)-$8PF_6$]$^+$ 1511.3 (calcd 1510.7); UV (λ nm, acetone) 420 vbr, 544 br.

Using a mixture of the free base 1,4-dioxybenzene (2,4,4,2) porphyrin isomers **11a** (61 mg, 4.21×10^{-5} mol) and **12a** (40 mg, 2.76×10^{-5} mol), together with **13** (188 mg, 2.66×10^{-4} mol), 1,4-bis(bromomethyl)benzene (88 mg, 3.33×10^{-4} mol), under the same reaction conditions as above, produced a mixture of products. Attempted purification was carried out by column chromatography (silica) by eluting initially with CH_2Cl_2/MeOH (10%), then MeOH/2M NH_4Cl solution/$MeNO_2$ (7 : 2 : 1 v/v) to obtain isomeric mixtures of α,β- and α,α-[2]-catenane fractions **15a** and **16a** in a ratio of ca. 3 : 2 (from NMR) as a dark purple solid (42 mg, 23%), mp 200–204 °C (from acetone/^{i}Pr$_2$O). The NMR spectrum of the mixture was a sum of the spectra of the individual components isolated above. This was followed by MeOH/2M NH_4Cl solution/DMF (4 : 5 : 2 v/v) to obtain isomeric mixtures of α,β- and α,α-[3]-catenane fractions **17a** and **18a** in a ratio of *ca*. 3 : 2 (from NMR) as a dark purple solid (10 mg, 4%), mp 234–237 °C (from acetone/^{i}PrOH). The NMR spectrum contained all of the peaks of the individual components isolated as above, together with broad peaks presumed as arising from polymeric non-porphyrinic material.

Acknowledgements

We thank the Australian Research Council for funding for this project, and the Royal Society of Chemistry for funding through a Journals Grant for International Authors.

References

1 A. R. Pease, J. O. Jeppesen, J. F. Stoddart, Y. Luo, C. P. Collier and J. R. Heath, *Acc. Chem. Res.*, 2001, **34**, 433; J.-M. Lehn, *Angew. Chem., Int. Ed. Engl.*, 1988, **27**, 89; V. Balzani, A. Credi and M. Venturi, *Chem. Eur. J.*, 2002, **8**, 5525.
2 V. Balzani, M. Gómez-Lopez and J. F. Stoddart, *Acc. Chem. Res.*, 1998, **31**, 405; V. Balzani, A. Credi, F. M. Raymo and J. F. Stoddart, *Angew. Chem. Int. Ed.*, 2000, **39**, 3349.
3 B. L. Feringa, *Acc. Chem. Res.*, 2001, **34**, 504; J. F. Stoddart, *Chem. Aust.*, 1992, 576; J. F. Stoddart, *Acc. Chem. Res.*, 2001, **34**, 410.
4 J.-P. Sauvage, *Acc. Chem. Res.*, 1998, **31**, 611.
5 D. B. Amabilino, P. R. Ashton, M. Belohradsky, F. M. Raymo and J. F. Stoddart, *Chem. Commun.*, 1995, 751; P. R. Ashton, M. Blower, D. Philp, N. Spencer, J. F. Stoddart, M. S. Tolley, R. Ballardini, M. Ciano, V. Balzani, M. T. Gandolfi, L. Prodi and C. H. McLean, *New J. Chem.*, 1993, **17**, 689.
6 P. R. Ashton, L. Pérez-García, J. F. Stoddart, A. J. P. White and D. J. Williams, *Angew. Chem., Int. Ed. Engl.*, 1995, **34**(5), 571.
7 D. B. Amabilino, P.-L. Anelli, P. R. Ashton, G. R. Brown, E. Cordova, L. A. Godinez, W. Hayes, A. E. Kaifer, D. Philp, A. M. Z. Slawin, N. Spencer, J. F. Stoddart, M. S. Tolley and D. J. Williams, *J. Am. Chem. Soc.*, 1995, **117**, 11142.
8 P. R. Ashton, C. L. Brown, E. J. T. Chrystal, K. P. Parry, M. Pietraszkiewicz, N. Spencer and J. F. Stoddart, *Angew. Chem., Int. Ed. Engl.*, 1991, **30**, 1042.
9 D. B. Amabilino, P. R. Ashton, A. S. Reder, N. Spencer and J. F. Stoddart, *Angew. Chem., Int. Ed. Engl.*, 1994, **33**(4), 433; D. B. Amabilino, P. R. Ashton, A. S. Reder, N. Spencer and J. F. Stoddart, *Angew. Chem., Int. Ed. Engl.*, 1994, **33**(12), 1286; P. R. Ashton, R. Ballardini, V. Balzani, M. T. Gandolfi, D. J. F. Marquis, L. Pérez-García, L. Prodi, J. F. Stoddart and M. Venturi, *J. Chem. Soc., Chem. Commun.*, 1994, 177.
10 P. R. Ashton, V. Baldoni, V. Balzani, A. Credi, H. D. A. Hoffmann, M.-V. Martinez-Diaz, F. M. Raymo, J. F. Stoddart and M. Venturi, *Chem. Eur. J.*, 2001, **7**, 3482; P. R. Ashton, S. E. Boyd, A. Brindle, S. J. Langford, S. Menzer, L. Pérez-García, J. A. Preece, F. M. Raymo, N. Spencer, J. F. Stoddart, A. J. P. White and D. J. Williams, *New J. Chem.*, 1999, **23**, 587; M. Asakawa, P. R. Ashton, V. Balzani, A. Credi, C. Hamers, G. Mattersteig, M. Montalti, A. M. Shipway, N. Spencer, J. F. Stoddart, M. S. Tolley, M. Venturi, A. J. P. White and D. J. Williams, *Angew. Chem., Int. Ed. Engl.*, 1998, **37**, 333; P. R. Ashton, J. A. Preece, J. F. Stoddart, M. S. Tolley, A. J. P. White and D. J. Williams, *Synthesis*, 1994, 1344; Z.-T. Li, P. C. Stein, J. Becher, D. Jensen, P. Mørk and N. Svenstrup, *Chem. Eur. J.*, 1996, **2**, 624; D. J. Cárdenas, A. Livoreil and J.-P. Sauvage, *J. Am. Chem. Soc.*, 1996, **118**, 11980.
11 V. Balzani, A. Credi, S. J. Langford, F. M. Raymo, J. F. Stoddart and M. Venturi, *J. Am. Chem. Soc.*, 2000, **122**, 3542.
12 D. B. Amabilino and J.-P. Sauvage, *New J. Chem.*, 1998, 395; M. Linke, N. Fujita, J. C. Chambron, V. Heitz and J. P. Sauvage, *New J. Chem.*, 2001, **25**, 790; J.-C. Chambron, C. O. Dietrich-Buchecker, V. Heitz, J.-F. Nierengarten, J.-P. Sauvage, C. Pascard and J. Guilhem, *Pure Appl. Chem.*, 1995, **67**, 233; D. B. Amabilino and J.-P. Sauvage, *Chem. Commun.*, 1996, 2441.
13 L. Flamigni, A. M. Talarico, S. Serroni, F. Puntoriero, M. J. Gunter, M. R. Johnston and T. P. Jeynes, *Chem. Eur. J.*, 2003, **9**, 2649.
14 M. J. Gunter and M. R. Johnston, *J. Chem. Soc., Chem. Commun.*, 1992, 1163.
15 M. J. Gunter, D. C. R. Hockless, M. R. Johnston, B. W. Skelton and A. H. White, *J. Am. Chem. Soc.*, 1994, **116**, 4810.
16 M. J. Gunter and M. R. Johnston, *J. Chem. Soc., Chem. Commun.*, 1994, 829.
17 M. J. Gunter and R. N. Warrener, *Chem. Aust.*, 1997, 25.
18 I. Willner, E. Kaganer, E. Joselevich, H. Durr, E. David, M. J. Gunter and M. R. Johnston, *Coord. Chem. Rev.*, 1998, **171**, 261; L. Flamigni, A. M. Talarico, M. J. Gunter, M. R. Johnston and T. P. Jeynes, *New J. Chem.*, 2003, **27**, 551.
19 D. B. Amabilino, P. R. Ashton, C. L. Brown, E. Córdova, L. A. Godínez, T. T. Goodnow, A. E. Kaifer, S. P. Newton, M. Pietraszkiewicz, D. Philp, F. M. Raymo, A. S. Reder, M. T. Rutland, A. M. Z. Slawin, N. Spencer, J. F. Stoddart and D. J. Williams, *J. Am. Chem. Soc.*, 1995, **117**, 1271.
20 P. R. Ashton, D. Philp, N. Spencer and J. F. Stoddart, *J. Chem. Soc., Chem. Commun.*, 1992, 1124.
21 D. B. Amabilino, P. R. Ashton, J. F. Stoddart, A. J. P. White and D. J. Williams, *Chem. Eur. J.*, 1998, **4**, 460; P. R. Ashton, C. L. Brown, E. J. T. Chrystal, T. T. Goodnow, A. E. Kaifer, K. P. Parry, A. M. Z. Slawin, N. Spencer, J. F. Stoddart and D. J. Williams, *Angew. Chem., Int. Ed. Engl.*, 1991, **30**, 1039; P. R. Ashton, S. E. Boyd, C. G. Claessens, R. E. Gillard, S. Menzer, J. F. Stoddart, M. S. Tolley, A. J. P. White and D. J. Williams, *Chem. Eur. J.*, 1997, **3**, 788.
22 M. J. Gunter, M. R. Johnston, B. W. Skelton and A. H. White, *J. Chem. Soc., Perkin Trans. 1*, 1994, 1009.
23 M. J. Gunter, T. P. Jeynes, M. R. Johnston, P. Turner and Z. P. Chen, *J. Chem. Soc., Perkin Trans. 2*, 1998, **21**, 1945.
24 A. Osuka, F. Kobayashi and K. Maruyama, *Bull. Chem. Soc. Jpn.*, 1991, **64**, 1213; A. Osuka, T. Nagata, F. Kobayashi and K. Maruyama, *J. Heterocycl. Chem.*, 1990, **27**, 1657.
25 The addition of Cs_2CO_3 to the reaction mixture was used to aid in the formation of this large porphyrin macrocycle *via* a cation templating effect—the so called 'cesium effect'.
26 J. E. Redman and J. K. M. Sanders, *Org. Lett.*, 2000, **2**, 4141.
27 P. L. Anelli, P. R. Ashton, R. Ballardini, V. Balzani, M. Delgado, M. T. Gandolfi, T. T. Goodnow, A. E. Kaifer, D. Philp, M. Pietraszkiewicz, L. Prodi, M. V. Reddington, A. M. Z. Slawin, N. Spencer, J. F. Stoddart, C. Vicent and D. J. Williams, *J. Am. Chem. Soc.*, 1992, **114**, 193.
28 *Dynamic NMR Spectroscopy*, ed. J. Sandstrom, Academic Press, New York, 1982, ch. 6; I. O. Sutherland, *Annu. Rep. NMR Spectrosc.*, 1971, **4**, 71.
29 This process was too fast to evaluate in the previous porphyrin [2]catenanes, but Stoddart[19] has found that this process occurs at a

rate of approximately 2.5×10^5 reorientations per second at ambient temperature for both the BPP40C12- and BPP46C14-based [2]catenanes, which are of a similar magnitude to **14b**. However, no value has been reported for the BPP34C10 [2]catenane **1b**, presumably indicating that the 'rocking' process occurs too fast in this catenane to be evaluated. The larger activation barrier for 1,4-dioxybenzene reorientation observed in **14b** over that observed for both the BPP40C12- and BPP46C14-based [2]catenanes may again reflect the short nature of the diethylene straps of the polyether chain linking the porphyrin and the 2HQ rings which would result in less flexibility, particularly in the presence of the porphyrin, to reorientate within the tetracation cavity.

30 However, we were not able to separate the catenane isomers given the solvent required for chromatography, *viz*. MeOH–2M NH_4Cl–$MeNO_2$ (7 : 2 : 1 v/v) for [2]catenanes and MeOH–2M NH_4Cl–DMF (4 : 5 : 2 v/v) for [3]catenanes.

31 Furthermore, the smaller shifts for the tetracation resonances for the [3]catenane isomers in comparison to the [2]catenane isomers upon catenane formation make good sense given that in order for the tetracation and bound HQ ring A to maintain π–π interactions with the porphyrin, then the second bound HQ and tetracation must move away from the porphyrin to allow this interaction, and supports the structure shown in Fig. 7. Hence, while one tetracation is shielded by the porphyrin and the other is deshielded, and because this would obviously be a dynamic process, then the average of these two environments would lead to a net smaller shielding of the tetracation protons for the [3]catenane isomers compared to their [2]catenane counterparts.

32 Additional processes that may be expected to occur include (i) a 'stacking, unstacking, shuttling and restacking' process involving an unstacking of the HQ-33 (ring B in Fig. 7) from the tetracation, bound HQ (ring A) and porphyrin subunits, followed by 'shuttling' of the tetracation to the second HQ ring A, and then restacking of the HQ ring B to the π-stacked superstructure; (ii) processes involving possible π–π interactions between the tetracation, HQ ring B, and porphyrin subunits (although this possible exchange process may not involve π–π interactions with the porphyrin, in order for process (ii) to occur, process (i) must also be involved, as the 'shuttling' between HQ rings A requires the intermediate 'shuttling' from HQ ring A to B as a 'stopover'); (iii) other processes with possible π–π stacking interactions between the tetracation, bound HQ ring B, and both HQ rings A (Fig. 7), without interaction with the porphyrin, although the NMR evidence suggests that such an arrangement is unlikely.